



Carbonate platform evolution of the Tirgan formation during Early Cretaceous (Urgonian) in the eastern Kopet-Dagh Basin, northeast Iran: depositional environment and sequence stratigraphic significance

Tayebeh Golafshani¹ · Mohammad Khanehbad¹ · Reza Moussavi-Harami¹ · Asadollah Mahboubi¹ · Amir Feizy²

Accepted: 28 September 2020

© Springer-Verlag GmbH Germany, part of Springer Nature 2020

Abstract

Tirgan formation of the Kopet-Dagh Basin (northeast Iran) represents one of the Urgonian carbonate platforms that were deposited during the Early Cretaceous time in the northern Alpine Tethys and deformed during the Alpine orogeny. In this study, six stratigraphic sections of the shallow-water platform sediments (Tirgan formation) were measured based on microfacies and fauna abundance. Detail study of petrography, fossil content, and sedimentary structures led to the identification of fifteen microfacies belonging to four facies belts including open marine, shoal, protected lagoon, and tidal flat. The sediments of the Tirgan formation exhibit calcareous green algae, abundant ooids, oysters, bryozoans, and crinoids in inner and middle platform ramp facies and planktonic bivalves and sponge spicules in outer-platform facies. Furthermore, the absence of basinal deposits and lack of evaporate evidence point to deposition under warm-temperate and humid climate conditions. Sequence stratigraphy analysis of Tirgan formation led to distinguish a single depositional sequence in all of the sections which are composed of transgressive and highstand systems tracts with sequence boundaries of type II (SB2). The lowermost lower Aptian Tirgan sequence in the study area relatively shows a similar trend in comparison with the global curve. This basin was deepened over time so that shaly and marly sediments of Sarcheshmeh formation were placed over Tirgan conformably and may suggest a drowning event that was likely related to unusual global warming. Last, this study contributes to the better understanding of the high distribution of facies assemblages in the Urgonian carbonate platforms.

Keywords Urgonian · Tirgan formation · Depositional environment · Sequence stratigraphy

Introduction

During the Barremian–Aptian, because of favorable geographical location and warm climate, the typical Early Cretaceous shallow carbonate facies that is known as Urgonian facies, was widely distributed on both sides of the Tethys (Fig. 1). Tirgan formation as one of the Urgonian platform deposited in north Tethys, the Kopeh-Dagh basin during the Early Cretaceous. The Kopeh-Dagh basin subsided during Jurassic to the latest Cretaceous

time, when it was connected, Turkmenistan and northern Afghanistan to the Caspian Basin (Afshar-Harb 1979; Buryakovsky et al. 2001; Ghorbani 2019). This basin was shaped in Middle Triassic, during the Early Kimmeridgian orogenic phase. Sedimentation has been continued from Jurassic to Miocene and sedimentary rocks consisted of five transgressive and regressive sequences (Moussavi-Harami and Brenner 1992). The sedimentary sequences Early Pliocene and has formed several anticlines and synclines with the northwest-southeast strike. The Early Cretaceous carbonates in the Kopet-Dagh Basin constitute one of the potential petroleum reservoirs. Based on paleontological and stratigraphic studies in the Lower Cretaceous, the part belonging to Hauterivian–Aptian was named Tirgan formation and is the reservoir rocks of gas (Afshar-Harb 1979). Primarily previous work on

✉ Mohammad Khanehbad
mkhanehbad@ferdowsi.um.ac.ir

¹ Department of Geology, Faculty of Science, Ferdowsi University of Mashhad, Mashhad, Iran

² National Iranian Oil Company, Exploration Directorate, Tehran, Iran

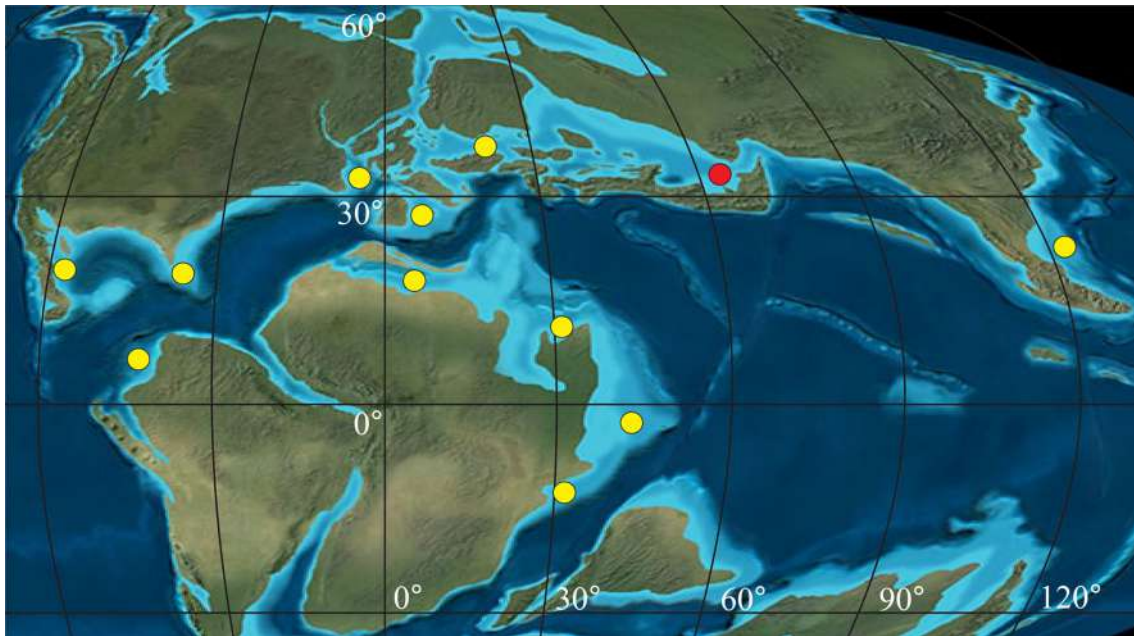


Fig. 1 Palaeogeographic map of the Late Barremian-Early Aptian showing the locations of the Urgonian carbonate platforms (yellow dots) and the studied area (red dots) (modified after Ron Blakey, NAU Geology, <http://deeptimemaps.com/global-series>)

the Tirgan formation in the Kopet-Dagh Basin has been the subject of many types of research (Kalantari 1969; Afshar-Harb 1979; Khodaei 1991; Aharipour 1996; Immel et al. 1997; Khazaei 2000). Recently detailed work has focused on the stratigraphy, biostratigraphy sedimentology, geochemical and reservoir quality of this platform succession (Taherpour Khalil Abad et al. 2013; Sharafi 2012; Javanbakht et al. 2013, 2018; Carevic et al. 2013; Molaei et al. 2019; Yavarmanesh et al. 2017; Abbassi et al. 2018; Tabatabaee et al. 2018; Bucur et al. 2019; Gheiasvand et al. 2019). These studies have provided the basic information related to the regional bio- and lithostratigraphical setting of the Tirgan carbonate platform. This platform is mainly ramps and its lack of frame-building organisms capable of building a steep-margined platform. To assess this model, we describe six sections through the Early Cretaceous Tirgan formation in the eastern Kopet-Dagh Basin (Fig. 2) and use architecture and geometry to propose and reconstruct the lateral and vertical facies changes and delineate sequence stratigraphy of this carbonate platform and to reconstruct its sedimentary evolution. Furthermore, we believe that studying the sedimentary environment and sequence stratigraphy of the Tirgan formation as a reservoir potential in the Kopet-Dagh sedimentary basin can provide, while answering some of the questions and ambiguities in the region, important information for future modeling of sedimentary basin and reconstruction

of environmental conditions of Urgonian platform carbonates during the Early Cretaceous.

Geological setting

The Kopet-Dagh region comprises fold, thrust Belt Mountains in northeastern Iran, and is believed to be the northern part of the Paleo-Tethys suture line (Stöcklin 1977; Alavi 1991; Robert et al. 2014). By collision of the Middle Iranian Plateau (MIP) with Northern Iranian Plateau (NIP) during the Middle Triassic and closure of the Paleo-Tethys basin, this region acted as an intracontinental subsidence basin during Middle Jurassic (MJ) to Middle Eocene (ME) time, while its sedimentary environments were controlled by WSW-ESE strike-slip faults (Afshar-Harb 1979). Horst and grabens formed in the region by these faults. In the area north of the village of Rezvan, a series of horst and graben occurs in a wide syncline with the Shurijeh formation in the core. In the west Kopet-Dagh, a small graben formed in the Garmab anticline during the deposition of the Tirgan formation (Afshar-Harb 1979). The Tirgan formation is characterized by thick-bedded oolitic to bioclastic limestone accompanied by thin layers of marly limestone, marl, and shaly limestone intercalations in the type section. The thickness of the Tirgan formation changes from less than 20 m in the east of Kopet-Dagh to more than 780 m at the type section (Afshar-Harb 1979) and in the West Kopet-Dagh the Tirgan formation thins rapidly (Fig. 2c). In the study areas of

this formation overlies Shurijeh formation, a fluvial succession (Moussavi-Harami and Brenner 1990; Hosseinyar et al. 2018), and is overlain by Sarcheshmeh formation consists of ammonite bearing shale and marl (Afshar-Harb 1979). In central Kopet-Dagh Basin, the Tirgan formation belongs to the upper Barremian through the lower Aptian interval (Afshar-Harb 1979; Immel et al. 1997; Carevic et al. 2013; Taherpour Khalil Abad et al. 2013). Gheiasvand et al. (2019) presented the new biostratigraphic data to assign a Berriasian (?)–Valanginian to Albian age in the type section. In the eastern part of eastern Kopet-Dagh, however, the Tirgan is classified as a lower Aptian succession (Kalantari 1969; Afshar-Harb 1979; Immel et al. 1997).

Material and methods

Six stratigraphic sections of the Tirgan formation of Urganian carbonate platforms (Figs. 1, 2) have been selected and measured along the northern Tethyan carbonate ramp so that from the east to west they include the Shurijeh, the Baghak, the Padeha, the Mozduran, the Ghorghoreh, and the Derakht-e Bid. Fieldwork forms the basis for studying sedimentary deposits so that 234 samples in total were taken and their thin sections were studied. Criteria studied in outcrops and thin sections are lithology, texture, rock color, bedding, sedimentary structures, fossils, and biogenic structures. Carbonate components percentages (the grains and matrix) were estimated using visual percentage charts (Flügel 2010). The carbonate classification was used in the scheme of Dunham (1962) and Embry and Klovan (1971). Facies types, depositional settings, interpretation of depositional environment have been based on using the standard models of Wilson (1975) and Flügel (2010) and Read (1985) and Burchette and Wright (1992) and Arnaud-Vanneau and Arnaud (2005). The recognition of 3-order depositional sequences was carried out by Van Wagoner et al. (1990), Vail et al. (1991), Catuneanu (2006), and Catuneanu et al. (2009).

Lithostratigraphy

The Tirgan formation is formed mainly of oolitic and bioclastic (mostly *Orbitolina*) limestone with subordinate layers of marl and calcareous shale. This name derives from the village of Tirgan, 40 km southeast of the town of Darrehgaz, in east Kopet Dagh. Regarding the difficult accessibility of the type locality, a paratype section is also introduced in the West Kopet Dagh, west of the village of Jozak by Afshar-Harb 1979 and as Urganian carbonate platforms by Taherpour Khalil Abad et al. 2013. In the Shurijeh (11 m thick), Baghak (14 m thick), Padeha (15 m thick), Mozduran (43 m thick), Ghorghoreh (42 m thick) and Derakht-e Bid

(35 m thick) sections (the eastern Kopet Dagh Basin) the Tirgan formation can be divided into two units based on the morphology and lithology (Figs. 3, 4, 5c). The lower unit forming badland topography disappears towards the east basin and is not observed in the Shurijeh section (Fig. 12). The upper unit which is a thick carbonate unit forms cliffs (Fig. 5a, b). But on the east is thin and does not affect the morphology area (Fig. 5c) which is probably due to the proximity to the Aghdarband tectonic windows (Fig. 14d) (Zanchi et al. 2016; Brunet et al. 2017). In the west of sections (Mozduran, Ghorghoreh, and Derakht-e Bid), Tirgan formation conformably over- and underlies the Shurijeh and Sarcheshmeh formations (Figs. 3, 12). But in the east of sections (Padeha, Baghak, and Shurijeh) faultily underlies the Shurijeh formation (Fig. 12). The lower unit of these sections consists of medium pale orange and grey calcarenite (Fig. 5d, e, f) and calcirudite (shell bed) with an alternation of red and green shales and grey calcilutite (Figs. 5e, 12l). Calcirudite contains 2–5 cm sized mud clast and bioclasts (mostly oyster and bryozoan) (Figs. 6b, f, 11b, 12a, d). The upper unit consists of cream and grey calcarenite (oolitic limestone) and calcirudite (Figs. 6a, c–e, 9e, 10b) with an alternation of grey calcilutite (marly limestone). The macrofauna, bivalves, echinoids, and gastropods (Fig. 6b, d) and cross-lamination, cross-bedding, trough-bedding hummocky cross-bedding (Fig. 9h), normal graded-bedding (Fig. 10b) and trace fossil (*Protovirgularia*) are sedimentary structures in these units (Fig. 7).

Biostratigraphy

During the Barremian-lower Aptian (Lower Cretaceous), the benthic foraminifer (orbitolinids), calcareous algae, coral, gastropods, bryozoans, and bivalves assemblages in Urganian carbonate environments of the Paleo-Tethyan realm is deposited (Arnaud-Vanneau and Arnaud 2005; Taherpour Khalil Abad et al. 2013). Base on primary micropaleontological studies from calcareous algae and benthic foraminifera assemblage (Kalantari 1969; Afshar-Harb 1979; Immel et al. 1997), the age of the Tirgan formation is Barremian to Aptian. But in recent micropaleontological studies, Gheiasvand et al. (2019) applying carbon isotope chemostratigraphy and benthic foraminifera and planktonic organisms in type section have established a new biostratigraphic data for the Tirgan formation (Berriasian (?)–Valanginian to Albian age). Molaei et al. (2019) based on ammonite assemblages in the west of Kopet-Dagh and Bucur et al. (2019) mainly the orbitolinid association was assigned a latest Barremian-early Aptian age to Tirgan formation. Based on these authors, four calcareous algae and six benthic foraminiferal (orbitolinid) assemblages were determined (Fig. 8). The age of the Tirgan formation along the studied sections provide the Aptian age.

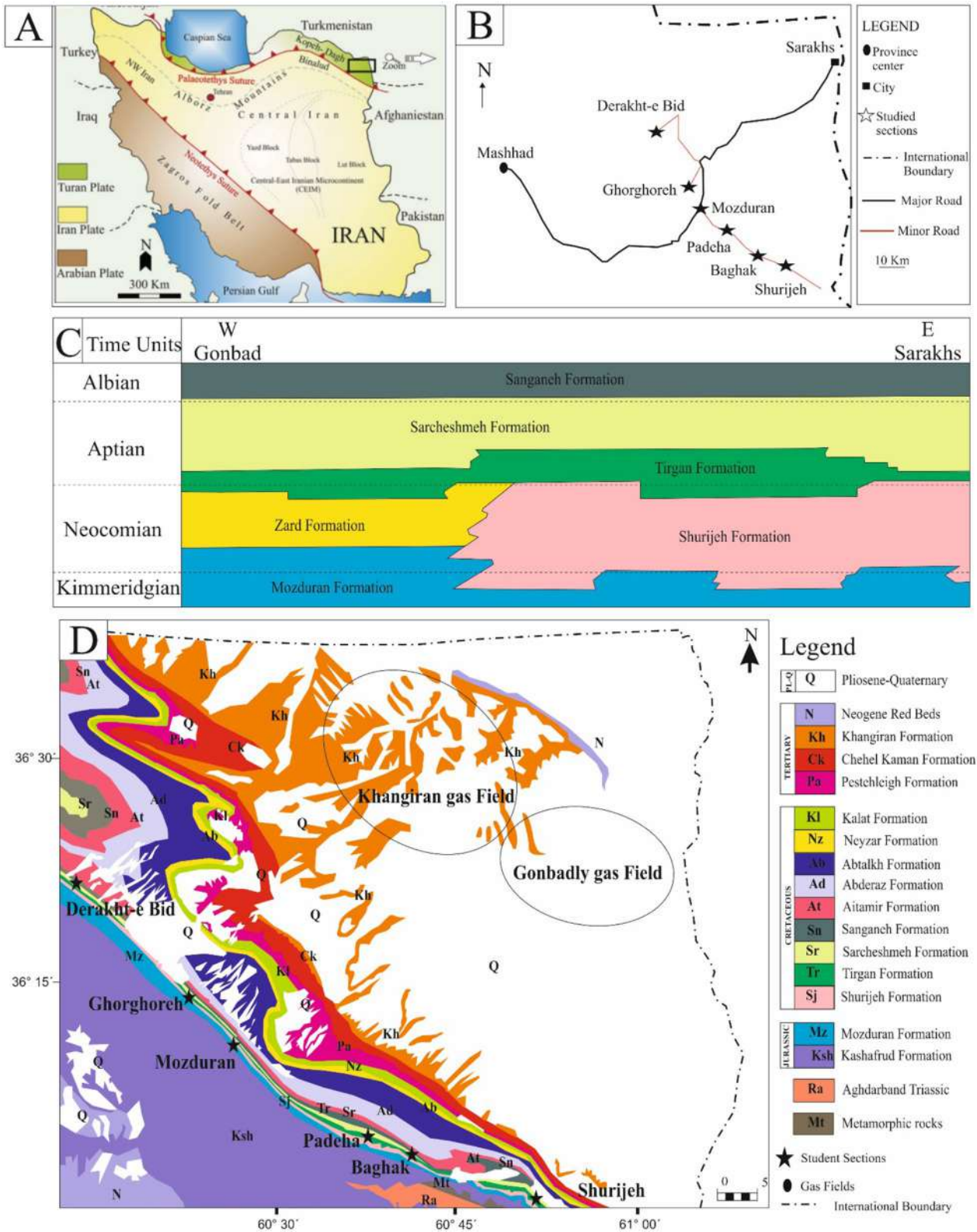


Fig. 2 Location map of the study area and measured stratigraphic sections in the Kopet-Dagh Basin. **a** Map of present-day Iran showing the geographical domains as well as the main sutures and tectonic structures including the Arabian plate, Iran plate, and Turan plate, moreover, a close-up view of the square of the study area in the SE Kopet-Dagh Basin (modified after Alavi 1991). **b** Close-up view of the locations of measured sections in the study area. **c** The chart illustrates lateral changes from the Sarakhs area in the far east to the Gonbad area in the far western part of the Kopet-Dagh Basin and (**d**) geology map of the study area (modified after Afshar-Harb 1982) 1: West of 1: Shurijeh, 2: Baghak, 3: Padeha, 4: Mozduran pas, 5: Ghorghoreh, 6: Derakhet-e Bid (source: author)

Facies analysis

The thickness and lithology of Tirgan formation are very variable in the studied sections. This formation consists mainly of oolitic limestone, limy sandstone, shale/marl, and shale. Field and detailed petrographic investigation using the microfacies approach has led to the recognition of fifteen facies types that characterize ramp platform development. These facies belong to four facies association (A, B, C, and D), which they are as follows:

Open marine (A1–A3)

Bioturbated mudstone (A1)

This microfacies is composed of thin to very thin-bedded (Fig. 9a) intercalated with marly limestone that contains very fine quartz silt, pyrite, burrow (Fig. 9b), and scattered bioclasts (planktonic bivalves and sponge spicules) (Fig. 9a, b). This facies can be observed sporadically in the western parts of the study area, upper parts of Mozduran, and Ghorghoreh sections.

Bioclast wacke-to floatstone (A2)

Oysters (~10%) and bryozoans (~8%) with sizes > 3 mm are the main components of this facies (Fig. 9c–e). Brachiopods, corals, and scattered serpulid tubes constitute the minor components (< 5%). Ooids, intraclasts, corticoid, and oncolid (mainly bryooncolids) also present (~5%). The mixture of complete and broken or complete shells (Figs. 6d, e, 9e) is characterized by thin-bedded grey limestone with fining-upward. This facies is observed in the upper parts of Padeha, Mozduran, and Derakhat-e Bid sections (mainly west of the study area).

Ooid bioclast pack-to rudstone (A3)

This grain-supported facies is mostly composed of ooids with radial-concentric structure (~22%) and bioclasts (~29%). Skeletal grains are bryozoans (~11%), echinoderms (~5%), oyster (~7) with sizes up to 3 mm, and other

skeletal grains (~6%). Intraclasts, peloids, cortoids, aggregates, oncoids, and quartz form about 8% of grains. In some samples of Baghak and Shurijeh sections, the number of ooids increases, and the name of this microfacies changes to ooid packstone with the erosional base, normal graded-bedding, and may display hummocky cross-stratification (Fig. 9f, h, i). It is the most abundant facies of open marine in the facies association and is observed in almost all sections (east to west of the study area).

Interpretation

According to the presence of horizontal lamination (Fig. 9a), lime-mud supported texture and existence of sponge spicules and planktonic bivalves (Fig. 9b), bioturbated mudstone microfacies has probably been occurred in a low energy environment in distal open marine setting (Bover-Arnal et al. 2009; Flügel 2010) and pyritization suggests deep-water dysoxic conditions at below the SWB (Payros et al. 2010; Bassi and Nebelsick 2010). Stenohaline fauna (bivalves, brachiopods, and echinoids) in microfacies bioclast wackestone/floatstone and ooid bioclast pack-to rudstone indicate proximal normal marine conditions (Flügel 2010; Bai et al. 2017). Components such as crinoids, brachiopods, bryozoans, and bivalves typically are in the photic zone in the middle and outer ramp sediments deposited (Burchette et al. 1990; Bai et al. 2017). Ooids and intraclasts as non-skeletal allochems in this facies have been probably transported from high-energy (such as shoals) to this environment by currents. Accumulations of shells fragmentation (especially bivalves) and the upward-fining are probably caused by various processes including current concentrations, storm wave, and tempestite concentrations (Rubert et al. 2012; Bover-Arnal et al. 2009; Laya and Tucker 2012). The lack of evidence for turbidity currents and shell concentrations is very common in mid-ramp settings so that suggests the deposition between the FWB and the SWB (Bover-Arnal et al. 2009; Bassi and Nebelsick 2010; Laya and Tucker 2012). According to the concentration of shell fragments (Fig. 9e), inverse texture (sorted ooid in micrite matrix), an erosional base (Fig. 9f), normal graded-bedding and hummocky cross-stratification (Fig. 9h, i) are interpreted as storm depositional and tempestite (Fursich and Oschmann 1986; Perez-Lopez and Perez-Valera 2012; Chatalov 2013).

Shoal facies association (B1–B3)

The grainstone shoal facies is pale to grey color, medium bedded, and in some beds are present lamination and cross-bedding (Figs. 7a, b, 10g, h).

Fig. 3 Field aspects of the Tirgan formation along the Mozduran section (as representation from the west of sections). The sequence stratigraphic subdivisions of the formation are shown by the green and blue triangles

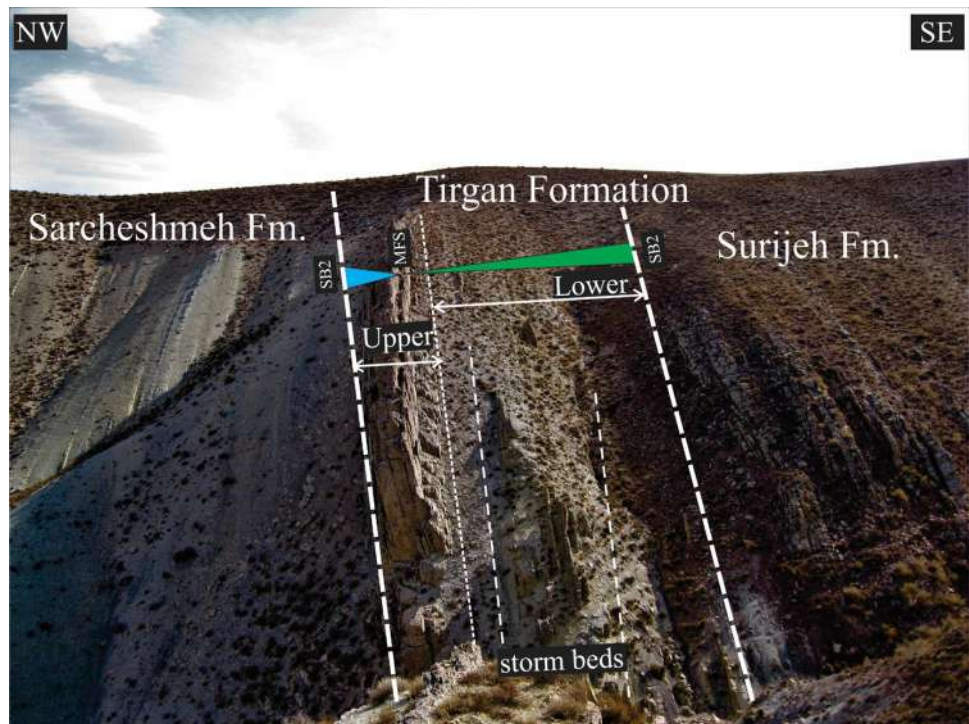
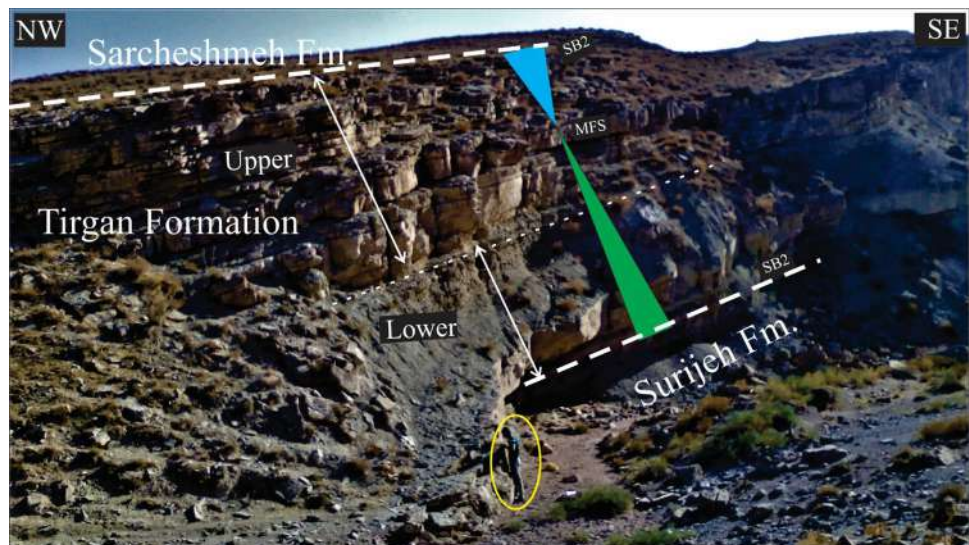


Fig. 4 Field aspects of the Tirgan formation along the Padeha section (as representation from the east of sections). The sequence stratigraphic subdivisions of the formation are shown by the green and blue triangles

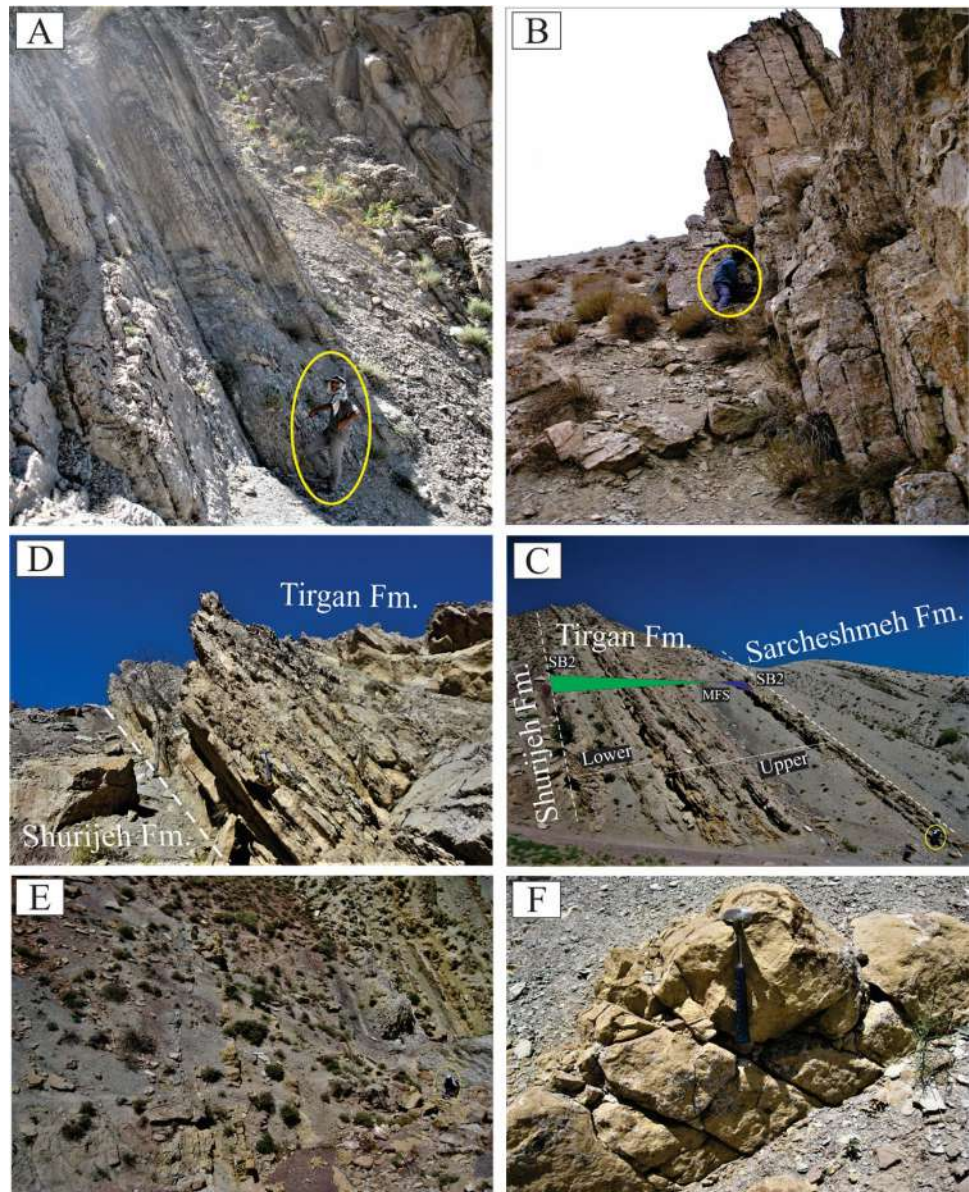


Bioclast ooid grainstone (B1)

Characteristic features of this microfacies are ooids with radial-distinct concentric structure (~23%) and size 0.2 mm and bioclasts are oysters (~6%), bryozoans (~4%) echinoderms, red algae (~4%), discoidal orbitolinids, and others allochems (6%) (Fig. 10a). Intraclasts, peloids, oncoid, and quartz form about 10% of grains. In some thin sections of Shuriyeh and Mozduran sections, the type of nonskeletal increases, and the name of this facies changes to bioclast/ooid intraclast grainstone (Fig. 10b–d). This

facies with a thickness of 0.3–0.8 m exhibit at the base of some shallowing upward cycles and the presence of normal graded-bedding (Figs. 7e, 10b, d). Pebbles with size ranges between 6 to 100 mm and roundness is floated in a matrix (~30–60%) that is formed by ooid/sand and carbonate cement. Clasts are mainly mudstone fragments but rarely milky white quartz is observed (Fig. 10b). It is the most abundant facies in the shoal facies association and is observed in almost all sections (east to west of the study area).

Fig. 5 Field aspects of the Tirgan formation. **a, b** The cliff formed in the Derakht-e Bid and the Mozduran sections, respectively, **c** the no cliff face in the Baghak section, **d** alternation of medium pale orange and grey calcarenite of the Baghak section, **e** alternation pale orange limestone and red and green shales and grey calcilutite in the first unit of the Mozduran section, **f** the pale orange limestone of the Mozduran section



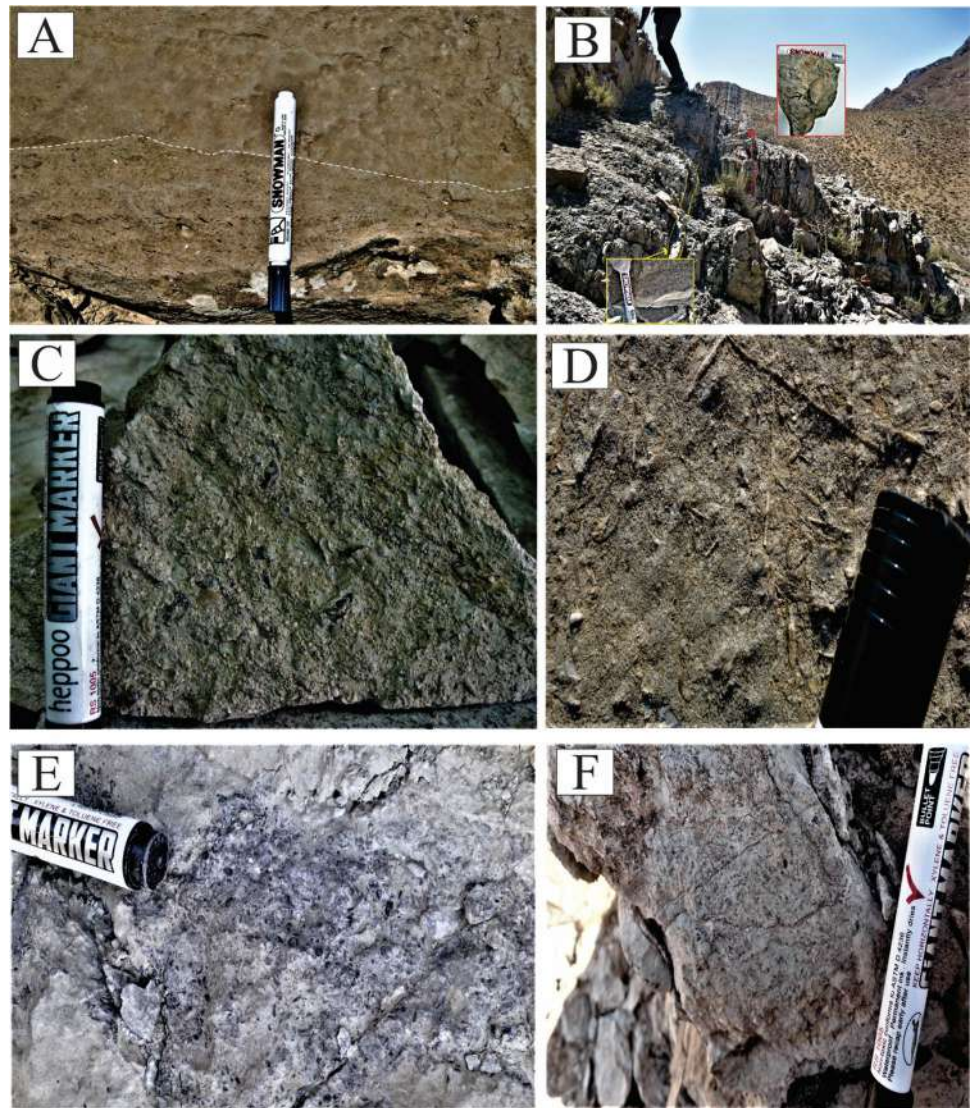
Well-sorted ooid grainstone (B2)

The ooids in grain-supported facies exhibit radial-concentric structures (~43%, 0.1–0.3 mm) and are well sorted (Fig. 10e). Most ooids are spherical to sub elongate and their shapes and thickness of the cortex often result from the shape of the nuclei. Aggregate grains of ooids and compound ooids are also present. Nuclei of ooids are common benthic foraminifers, peloids, debris shells, and quartz. This facies developed in Bahgak, Padeha, and Ghorghoreh sections (mainly east of the study area).

Bioclast peloid grainstone (B3)

These sediments are characterized by accumulations of very small (~0.2–0.4 mm), grain-supported, equal-sized peloids (~23%, probably fecal pellets) associated with benthic foraminifera (miliolids), Ostracods, green algae, few intraclasts, ooids, and conical orbitolinids (Fig. 10f). This microfacies is mostly common in the Mozduran (Fig. 5b), Ghorghoreh, and Drakht-e Bid (Fig. 5a) sections (west of the study area).

Fig. 6 Field photos of different types of shell beds in Tirgan formation in area study. **a** The sharp and erosional base and sharp top of the bioclast shell bed in the Ghorghoreh section, **b** two beds of bivalves and gastropods shell bed with different states of preservation that are in the lower bed complete and in the upper bed broken. **d–f** Slide view of bioclast shell bed in the Shurijeh, the Padeha, and Baghak sections, respectively

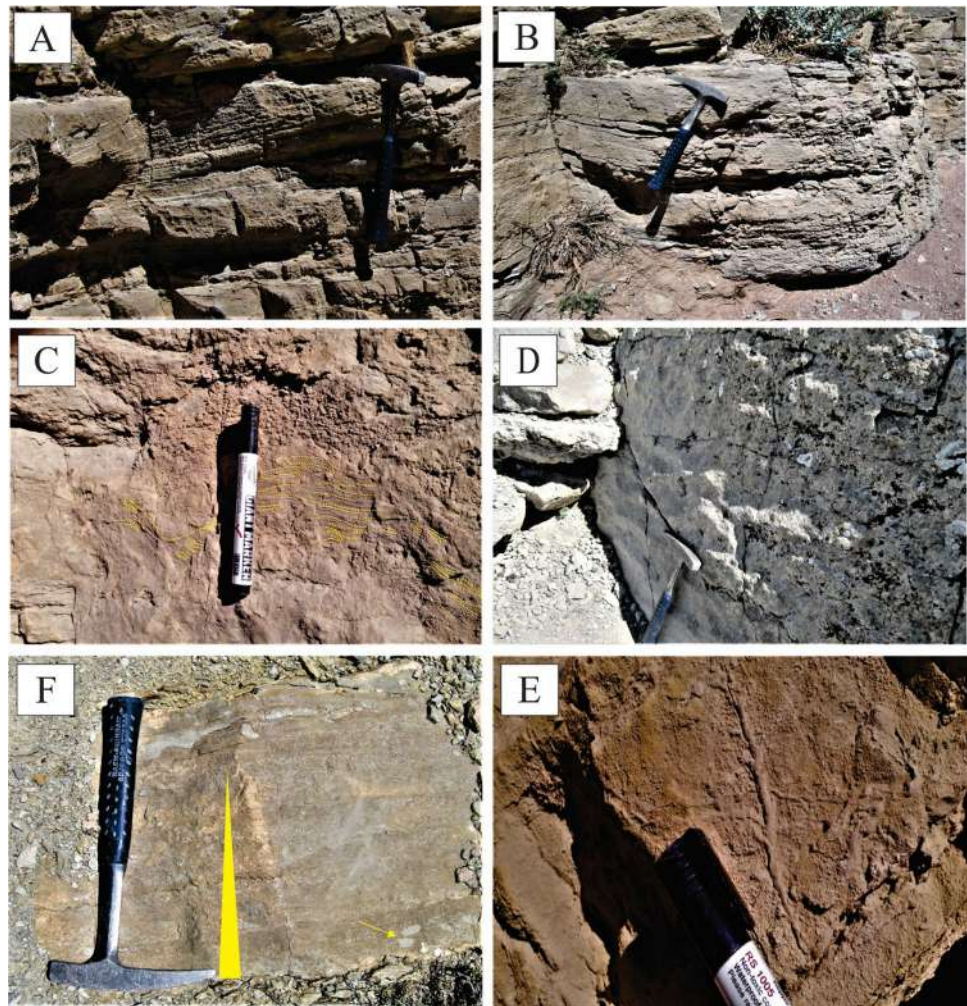


Interpretation

Accumulations with a relatively high percentage of stenohaline fauna (such as bryozoans and oysters) with ooids, intraclasts and lamination and cross-bedding (Fig. 10a) show that this microfacies may have occurred on or near the seaward edge of platforms and formed within the inner ramps at the depth of about 30–100 m due to the present bivalve, echinoderm and bryozoan fragments with grainstone in similar facies (Nelson et al. 1988; Pomar et al. 2001). Abundance ooids and also intraclasts and normal graded-bedding (Figs. 7e, 10b, d) in microfacies B1 (bioclast/ooid intraclast grainstone) properly occurred in high-energy environments of oolitic shoals and channels created by a storm or tidal currents (Adabi and Rao 1991; Łuczyński et al. 2014). Quartz grains are (Fig. 10b, c) abundant in this microfacies and indicative of a close of the source area (Miall 1997; Amir Hassan et al. 2013). Well-sorted grains and grain-supported, radial-concentric ooid,

cross-bedding and lamination in well-sorted ooid grainstone microfacies (Fig. 10f) indicate a high-energy shoal environment and deposited above the fair-weather wave base (Bachmann and Hirsch 2006; Palma et al. 2007; Bover-Arnal et al. 2009; Laya and Tucker 2012; Armella et al. 2013). The presence of ooids with cross-bedding in these facies evidenced their formation in saturated water shallow and warm concerning calcium carbonate (Betzler et al. 1997; Burchette et al. 1990; Purkis and Harris 2016). Additionally, the existence of peloid and lagoon fauna (miliolids and green algae), cross-lamination in bioclast peloid grainstone also suggest on the landward face of an oolitic shoal.

Fig. 7 Field photos of different types of sedimentary structures in Tirgan formation in area study. **a** Cross-bedding in the Padeha section, **b** cross-lamination in the Padeha section, **c** trough cross-bedding in the Padeha section, **d** wavy ripple mark in the Derakht-e Bid section, **e** normal graded-bedding in storm layers in the Ghrghoreh section, **f** trace fossil *Protovirgularia* in the Baghak section



Lagoon facies association (C1–C3)

Bioclast oncoid ooid packstone/wackestone (C1)

This microfacies consist of diverse skeletal grains including lagoonal (green algae, gastropods, benthic foraminifera, ~5%), and open marine (echinoids, bryozoans and bivalve fragments (~6%) fauna. Non-skeletal allochems mostly consist of ooids (~17%), in the wackestone facies about 5%, oncoid (~11%), and some intraclasts and peloids (3%). Quartz grains are very rare (1%) (Fig. 11a–c). In some samples (especially in the Ghorghoreh section), oysters (larger than 4 mm), are floated in a matrix (ranges from 30 to 60 percent) or peloids (2–19%), ooid (5–30%), and spray-micrite cement (Fig. 11b, c) with poorly sorted and densely packed. This facies with sizes > 3 mm bioclasts as shell beds (Figs. 6c, 11a) in field exhibit at the base of some deepening upward cycles and is defined by medium, grey to yellow limestone beds with erosional base, trough cross-bedding and wavy ripple (Fig. 7c, d)

in a few beds and is observed in almost all sections but is mainly developed in the western sections (Fig. 14).

Bioturbated bioclast wackestone/mudstone (C2)

Skeletal components include benthic foraminifera (mainly textularids, *Balkhania*, with rare presence of miliolids), green algae, ostracods, bivalves, and gastropods (~8–22%). Quartz grains are present in some samples (Fig. 11d). Bioturbations are mainly filled by dolomite (Fig. 11e). This facies is defined by medium, grey to yellow limestone beds (Fig. 5f) with trace fossil (*Protovirgularia*) (Fig. 7f) and is mainly observed in the western part of the study area (Mozduran, Ghorghoreh, Derakht-e Bid sections).

Bivalve boundstone/floatstone (C3)

Planktonic bivalves (~35), oysters (~9%), echinoderms and corals (~4%), ostracods, serpulid tubes, and gastropods (~5%) are the main components. The characteristic feature

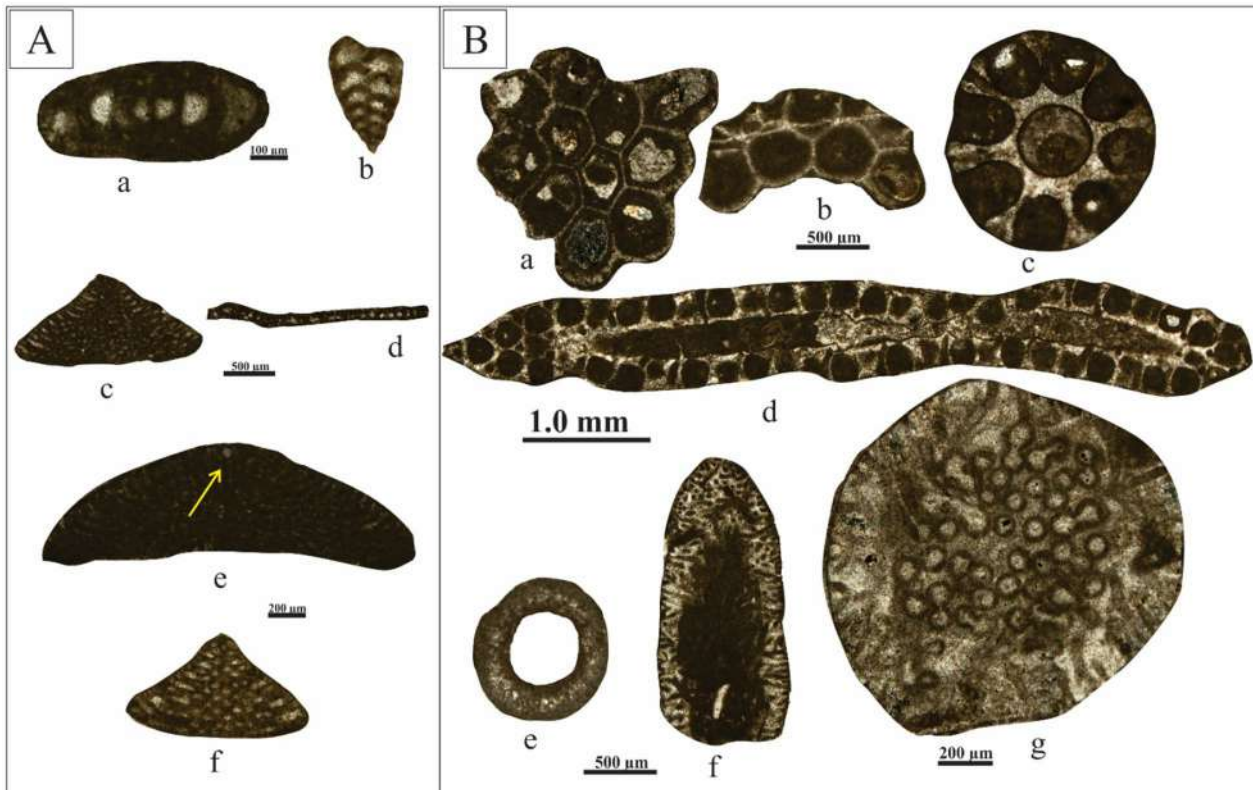


Fig. 8 Benthic foraminifers and Calcareous algae of the Tirgan formation in the studied area and their position in the section. **A** Benthic foraminifers: (a) *Nautiloulina oolithica*, in Ghorghoreh section, 4 m, Aptian, (b) *Vercorsella* aff., in Mozduran section, 39 m, Aptian, (c) *Iraquia* cf. *hensoni*, in Mozduran section, 42 m, Aptian, (d) *Balkhanina* cf. *balkhanica* in Ghorghoreh section, 22 m, Aptian, (e) *Praeorbitolina*?

P. transiens?, in Padeha section, 11 m, Aptian, (f) *Simplorbitolina* sp., in Mozduran section, 39 m, Aptian. **B** Calcareous algae: (a, b) *Kopetdagaria sphaerica*, in Mozduran and Padeha sections, 30 m and 5 m, respectively, Aptian, (c, d) *Montiella? elitzae*, in Mozduran and Padeha sections, 32 m and 2 m, respectively, Aptian, (e, f, g) *Boueina hochstetteri*, in Mozduran section, 31 m and 39 m, Aptian

of this microfacies is homogenous lime mud matrix and erosive-based (Figs. 6b, 11f–h) and is grey limestone and thin beds. Dolomite formed as a pore-filling (Fig. 11g, h). This facies is only observed in the Mozduran and Ghorghoreh sections (West of the study area).

Interpretation

The co-occurrence of lagoonal fauna (green algae, gastropods, miliolids) and normal marine fauna (echinoids, bryozoans, and bivalve) and the presence of nonskeletal ooid, peloid, and oncoid indicate that deposited in an open lagoon. The open marine and lagoonal mixed fauna may also be because of a connection between the lagoon and the sea (Singh 2012). The bioclast concentration and poorly sorted oyster remains with a sharp erosional base and trough cross-bedding and wavy ripple mark are identified lag concentration (Kidwell 1991) and probably indicate a high-energy inner ramp environment (on or near the landward edge of platforms) and deposited above the fair-weather wave base. The overall fine-grained nature indicates a low-energy

environment. The presence of ostracods together with small benthic foraminifera, green algae as restricted fauna, and bioturbation (trace fossil, *Protovirgularia*, Fig. 7f) suggest that deposited in a lagoon protected from ooid shoals. Dasycladacean green algae, which are also common, suggest deposition may have taken place in a very shallow marine environment (Curry 1999). In bivalve boundstone/floatstone facies, due to the mixing of open marine and lagoonal fauna with erosive-based, represent storm deposits in a Lagoon setting. Besides, the orientation of bivalves in this facies is probably due to the overpressure or the chemical compression (macrostylolites) (Fig. 11i).

Tidal flat facies association (D1–D4)

Sandy bioclast/ooid grain- to rudstone (D1)

This microfacies includes calcirudite limestones with grain size ranging from 0.5 to 4 mm in size (Figs. 6f, 12a–e). Coarse grains (larger than 2 mm) often contain various skeletal fragments (oysters, echinoderms, and others, 13%), and

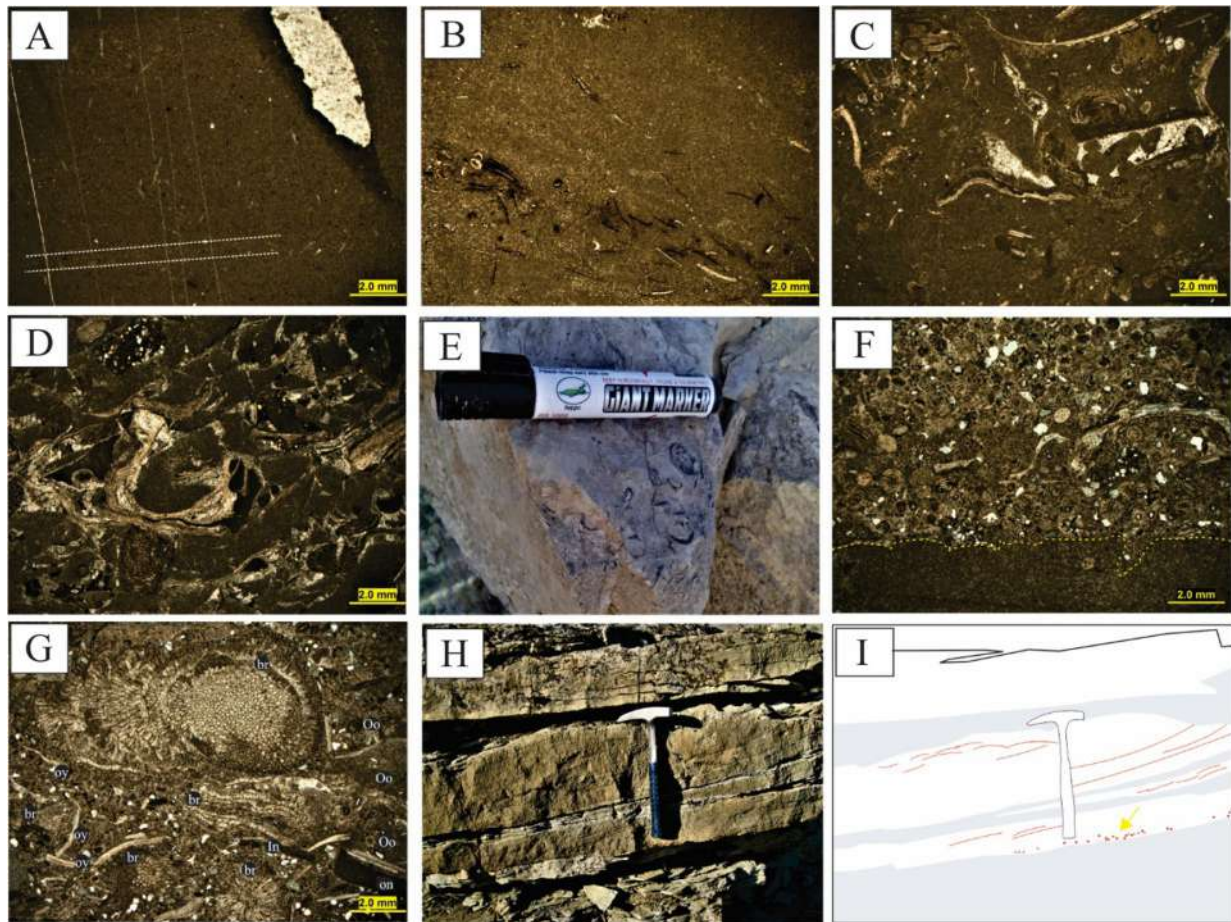


Fig. 9 Field photos and photomicrographs of the open marine facies. **a, b** Bioturbated mudstone microfacies with detail of burrowing and thin to very thin-bedded in **a**, bioturbation, and pritzation in **b–e** bioclast wackestone/floatstone microfacies, the arrow indicates a bryozoan ooid in **c**, with detail of complete or broken shells in the photomicrograph and the field aspects have shown, in **d, e** figs, respectively

(Padeha section). **f–i** ooid bioclast pack-to-rudstone microfacies with detail of inverse texture and an erosional base in **f**, bryozoans large clasts in **g**, hummocky cross-stratification, normal graded-bedding in **h** and **i** (Shurijeh section). *br* bryozoan, *oy* oyster, *In* intraclast, *Oo* ooid, *on* oncoid

intraclasts (~5%), which are floated in a matrix or coarse ooid (2–19%), quartz grains (5–30%), peloids (~1%), and spray-micrite cement. The erosional base, rarely cross-bedding, and an orientation in the fossils in the west of sections are the most important features in this facies. Also, the number of fauna increases from the east (Baghak, Padeha sections) (Fig. 12c–e) to the west (Mozduran, Ghorghoreh, and Derakht-e Bid) of the study area but quartz grains and ooids decreased (Fig. 12a, b).

Mudstone with fenestral (D2)

The characteristic feature in this microfacies is well developed fenestral fabrics (Fig. 12f) that comprises few Bioclasts and quartz grains and pale orange mudstones.

Fenestral voids are filled by dolomite or calcite with a mean of 1.2 mm in size. This facies developed in Mozduran and Baghak sections.

Limy sandstone (D3)

Limy sandstone is in the lowermost part of Mozduran, Ghorghoreh, and Derakhat-e Bid sections. The main components of this microfacies consist of mostly quartz grains (~38% and ranges between 0.1 to 0.6 mm in sizes), peloid and intraclast (~6%), few bioclasts (~5%), and few bent mica (muscovite) (Fig. 12g). The quartz grains are mostly monocrystalline with subangular to rounded and moderate to well sorted.

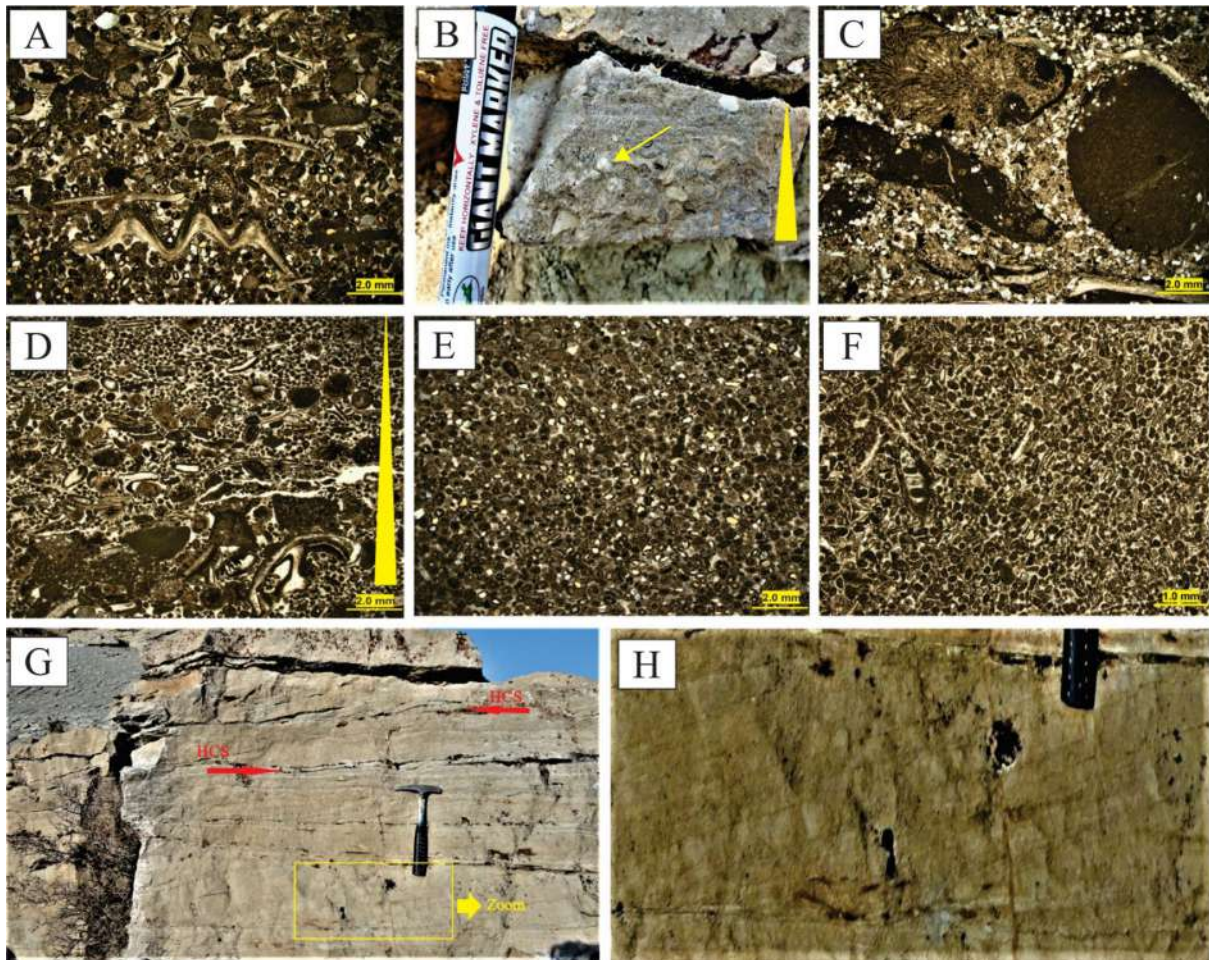


Fig. 10 Field photos and photomicrographs of the shoal facies. **a** Bioclast ooid grainstone microfacies, **b–d** bioclast/ooid intraclast grainstone microfacies that the field photo **b** and photomicrograph **c** are the same (Shurijeh section), with detail of normal graded-bedding or fining upward cycles in **b** and **d**, also arrow in **b** indicates a milky

white quartz pebble. **e** Sorted ooid grainstone microfacies, **f** bioclast peloid grainstone microfacies, **g** shallowing-upward cycle with lamination, HCS (hummocky cross-bedding), and **h** cross-bedding in beds of the grainstone shoal facies (Shurijeh section)

Heterolithic bedding or limy sandstone-mudstone (D4)

This microfacies consists of limy sandstone and mudstone and can be observed sporadically in Mozduran, Ghorghoreh, and Derakhat-e-Bid sections (in the west of the study area). Quartz grains (~20%) and bioclasts (~5%) are the main components of limy sandstone. Grain size is often fine sand (>0.1 mm), with medium roundness and well sorting. Also, flaser to wavy structures can be observed (Fig. 12h). Bioturbation has partially decayed lamination and sediment structures (Fig. 12i).

Interpretation

Sandy bioclast/ooid grain- to rudstone facies with an erosional base oriented fining-upward cycles and with a slightly lateral extension, presence of directing fossils

(Fig. 12a), and with distant lateral extension can indicate coastal channels formed in a storm or tidal currents (Tamura 2003). Fenestral porosity is of polygenic origin (Flügel 2010) due to the presence of bioturbation that can be interpreted as the most probable origin (Fig. 12f). The absence of structures (e.g., mud cracks) and the existence of fenestral porosity may have occurred in the intertidal setting (Flügel 2010). Based on the preservation of the mud matrix, the lack of fossil, interbedded of limy sandstone and red color with tidal evidence, it is interpreted to be deposited under lower energy conditions in coastal tidal flat (Fig. 12g) have been suggested in the tidal zone so that is often related to the alternation of bimodal tidal currents (Adnan et al. 2015). Flaser (Fig. 12h) beds or heterolithic bedding facies are related to alternation of bimodal tidal currents and continuous changes in energy conditions, intermediate high-energy

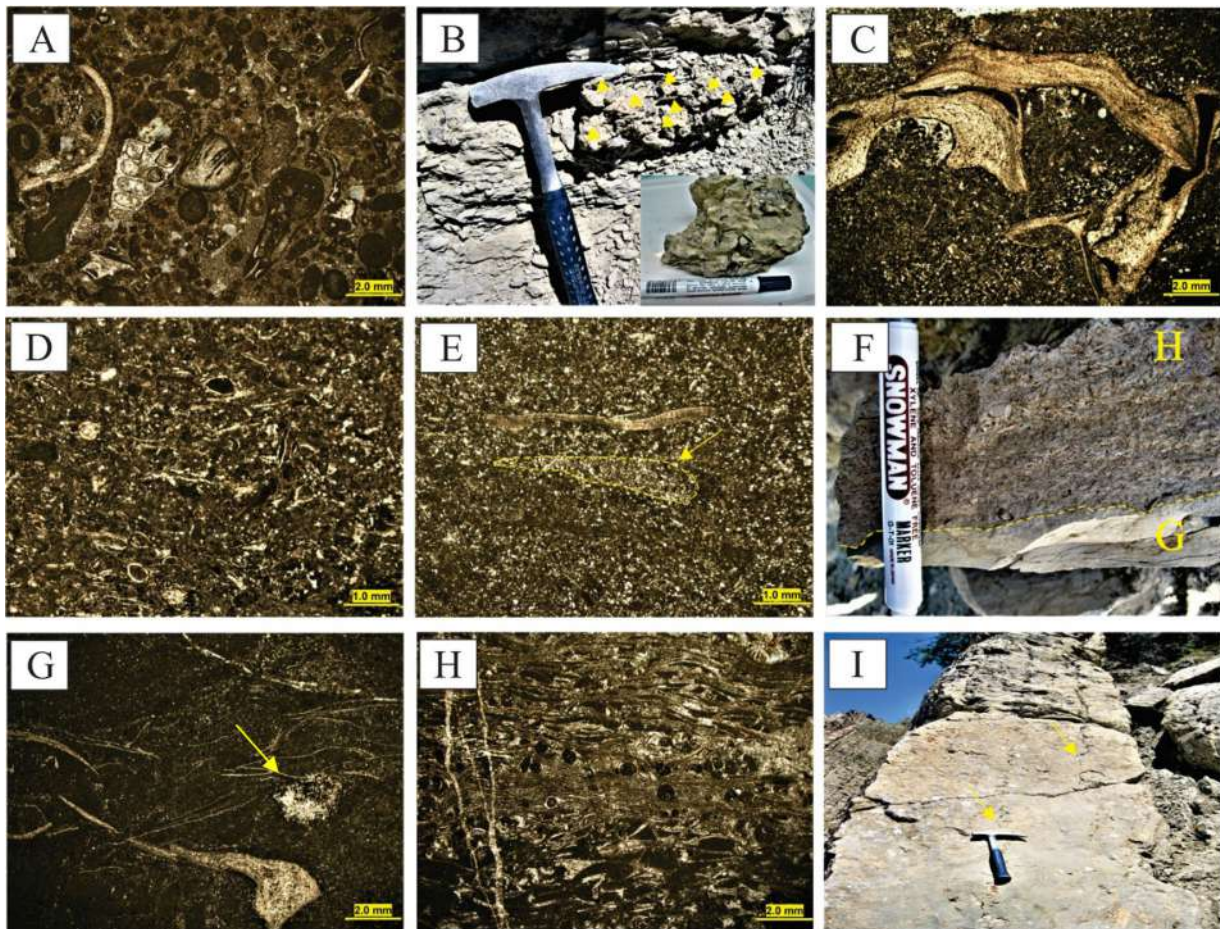


Fig. 11 Field photos and photomicrographs of the lagoon facies. **a–c** bioclast oncid ooid packstone/wackestone microfacies, that the field photo **b** and photomicrograph **c** are the same, arrows in **b** indicate oysters (Ghorghoreh section), **d** bioturbated bioclast wackestone microfacies, **e** bioturbated bioclast mudstone microfacies, the arrow indicates bioturbations that are mainly filled by dolomite, **f** bivalve

boundstone/floatstone microfacies with detail of erosion surface between **g** and **h** photomicrographs (Ghorghoreh section), **g** bivalve floatstone microfacies arrow indicates a vague that filled by dolomite, **h** bivalve boundstone/floatstone microfacies, **i** macrostylolite (Dera-kht-e Bid section)

facies (limy sandstone) and low energy (mudstone) in the intertidal setting have formed.

Fine-grained facies association (T1–T2)

Marly limestone (T1)

This facies occurs as interbeds with lagoonal and open marine facies in different parts of the sections (Fig. 14) and is observed grey, dark grey colors (Fig. 12j). Microfossils (e.g., echinoderms, oysters, and...) and nonskeletal (e.g., ooids) are distributed in the upper part of sections. Bioturbation is the most important sedimentary structure (Fig. 12k).

Calcareous shale (T2)

This facies can be mostly observed as interbeds in lower parts of the Mozduran and Ghorghoreh sections (Fig. 14) with gray to green and red–purple colors (Fig. 12l) that alternates with limy sandstone microfacies. The Calcareous shale is non-fossiliferous with thicknesses of less than 1.5 m.

Interpretation

Marly limestone with bioturbation and gray to green colored may indicate redox conditions probably in the tidal environment to a very shallow marine (e.g., Davis 2012). Based

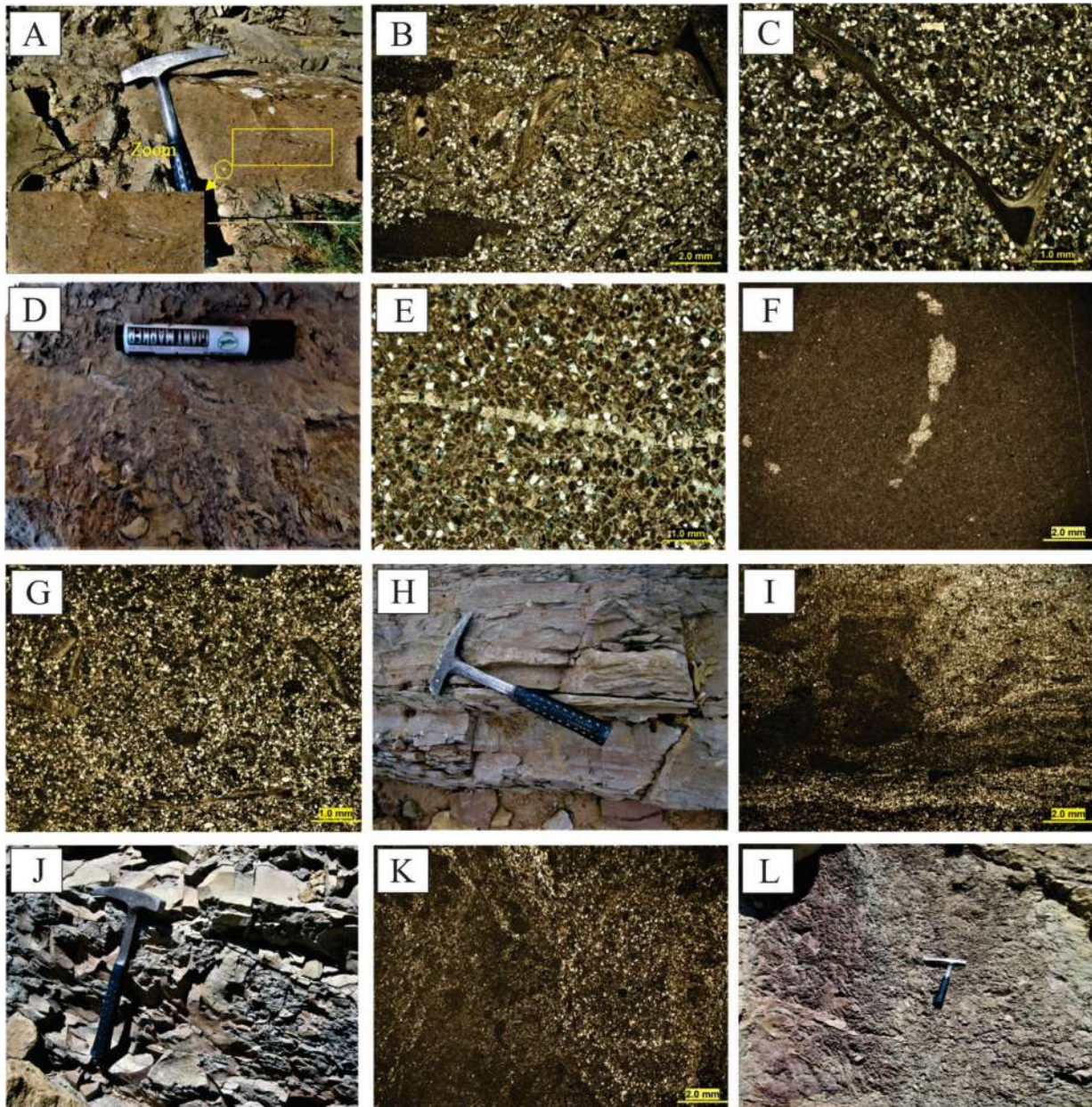


Fig. 12 Field photos and photomicrographs of the tidal flats and the fine-grained facies. **a, b** Sandy bioclast/oid grain- to rudstone microfacies with high quartz grains (Derakht-e Bid section) with detail photo **a** of directing fossils, **c–e** sandy bioclast/oid grain- to rudstone microfacies, with high many fauna and ooids **d** and **e** are the same

too (Baghak section), **f** mudstone microfacies with fenestral, **g** limy sandstone microfacies **h, i** heterolithic bedding or limy sandstone-mudstone microfacies (Mozduran section), **j** field photo of marly limestone microfacies (Mozduran section), **k** bioturbation in marly limestone microfacies, **l** green to red shale (Mozduran section)

on the red color in calcareous shale, the lack of fossil and interbedded with tidal flat facies deposited in the coastal tidal flat area.

Conceptual depositional models

The Early Cretaceous carbonate succession (Tirgan formation) forms part of a carbonate ramp in the study areas, in which sedimentation mostly occurred above the storm wave base belong to the inner ramp (Fig. 13). The facies belts in ramps are controlled primarily by energy levels (fair-weather wave base and storm wave base), variations in

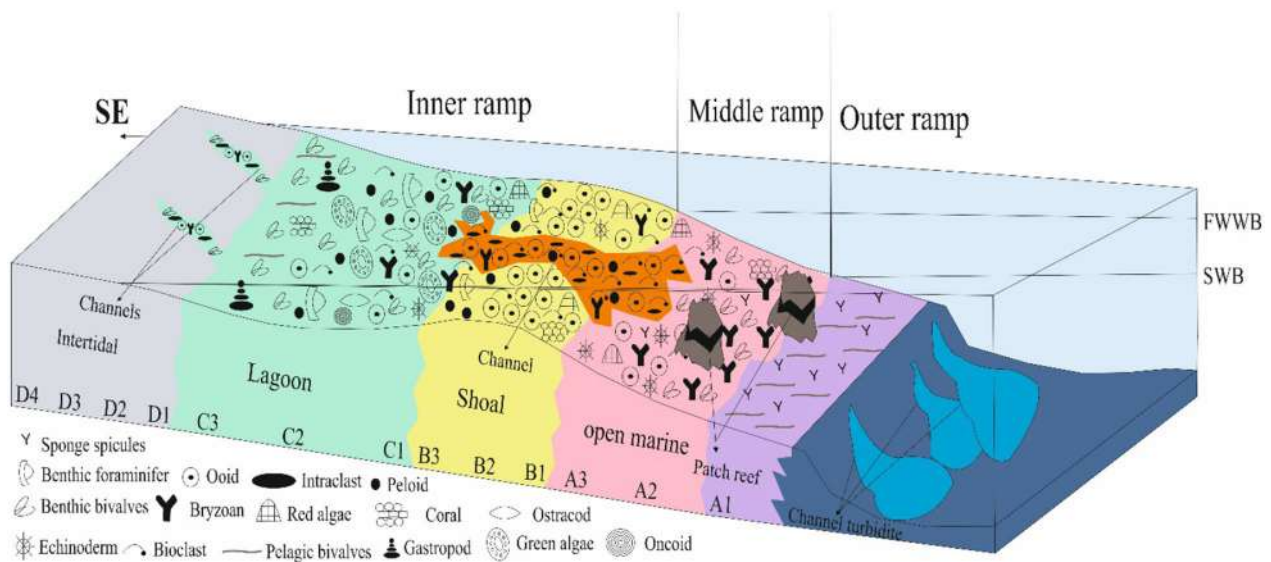


Fig. 13 Schematic model for carbonate platform environments of the Tirgan formation in the Kopet-Dagh Basin based on interpretation of facies belts, sedimentary environments, their lateral relationships,

and correlation with other sections. Distribution of fossils, facies, and their codes showed on the model. *FWWB* fair-weather wave base, *SWB* storm wave base

ramp topography (without a morphological break at the shelf edge), and material transport by storms, waves, and tides (Ahr 1973; Read 1985; Burchette and Wright 1992). Carbonate ramp environments are consisted of by (1) above fair-weather wave base, inner ramp, (tidal flat, D1–D4, Lagoon C1–C3, and shoal B1–B3 facies associations), (2) between fair-weather wave base and storm wave base, the middle ramp, (proximal open marine facies associations, A2–3), and (3) below normal storm wave base down the wave, the outer ramp, (distal open marine facies association, A1) and the basin (Burchette and Wright 1992). To reconstruct the depositional environment of the Tirgan formation, our study benefited from previous research in the Kopet-Dagh Basin. Aharipour (1996) in the northwest of the basin showed that the Tirgan formation in the Gharnaveh sections (80 m thick) (number 1 in Fig. 16a) is composed of alternating thin-bedded grey limestone, dark argillaceous limestone, and thick-bedded orbitolina limestone (Fig. 15a). Sedimentary structures including channel, graded bedding, cross-bedding and slump folding, and imbrication fabric are recognized and suggested as calciturbidite facies in the deeper environment. The study of the Tirgan formation in the west of Kopet-Dagh Basin by Tabatabaei (2012) shows that this formation in the TakelKuh (225 m thick) section in the northwest of the basin (numbers 2 in Fig. 16a), due to the alternation of pelagic and hemipelagic limestone and calciturbidite, suggested that are deposited in distal open marine or basin settings. She also introduced the environment of this formation in the Zav (580 m thick), the Khorkhud (410 m thick) and the Jozak (330 m thick), paratype section, (southwest of the basin, respectively numbers 3, 4, 5 in Fig. 16a) of an open marine,

barrier or shoal, lagoon, and tidal flat. It seems that there are conditions for coral growth in nearby areas. Therefore, patch reefs from these areas have been reported (Khazaei 2000). Tirgan formation in the central part of the Kopet-Dagh Basin, the Sisab (215 m thick, Taher Pour Khalil Abad 2013), the Radkan and the Chenaran (respectively, 238 and 119 m thick and numbers 7, 8 in Fig. 16a), Javanbakht et al. 2013) and the Tirgan (number 9 in Fig. 10a) (640 m thick, Gheivand et al. 2019), type section, is deposited of the shallow marine environment that is mostly composed of oolitic limestone. Generally, sedimentation of Tirgan formation in the Zavin section (110 m thick, Javanbakhat et al. 2011) (number 10 in Fig. 16a) and the studied area (numbers 11–16 in Fig. 16a), in the eastern basin, were formed in Tidal flat (intertidal) and subtidal environments mixed carbonate and siliciclastic that are attributed to the episodic influx of sediments from the terrestrial source or to mixing of sediments from different environments (Duncan et al. 2003). After correlation between different sections, the thickness of the Tirgan formation increases from the east toward the Tirgan village (type section) (e.g., 11 m in Shurijeh, 110 m in the Zavin, and 640 m in the Type sections). In some studies (e.g., Khodaei 1991), this abrupt increase in thickness has been interpreted to be related to the carbonate platform of a rimmed shelf type. But positions of the Radkan and the Chenaran sections (number 7, 8 in Fig. 16a) and the village of Tiregan (number 9 in Fig. 16a) in the central of basin appear that the origin of this increase in thickness must probably be related to a tectonic of area (of course requires tectonic studies in these areas?). Because they strongly differ from their thickness and have not been reported reef builders such as

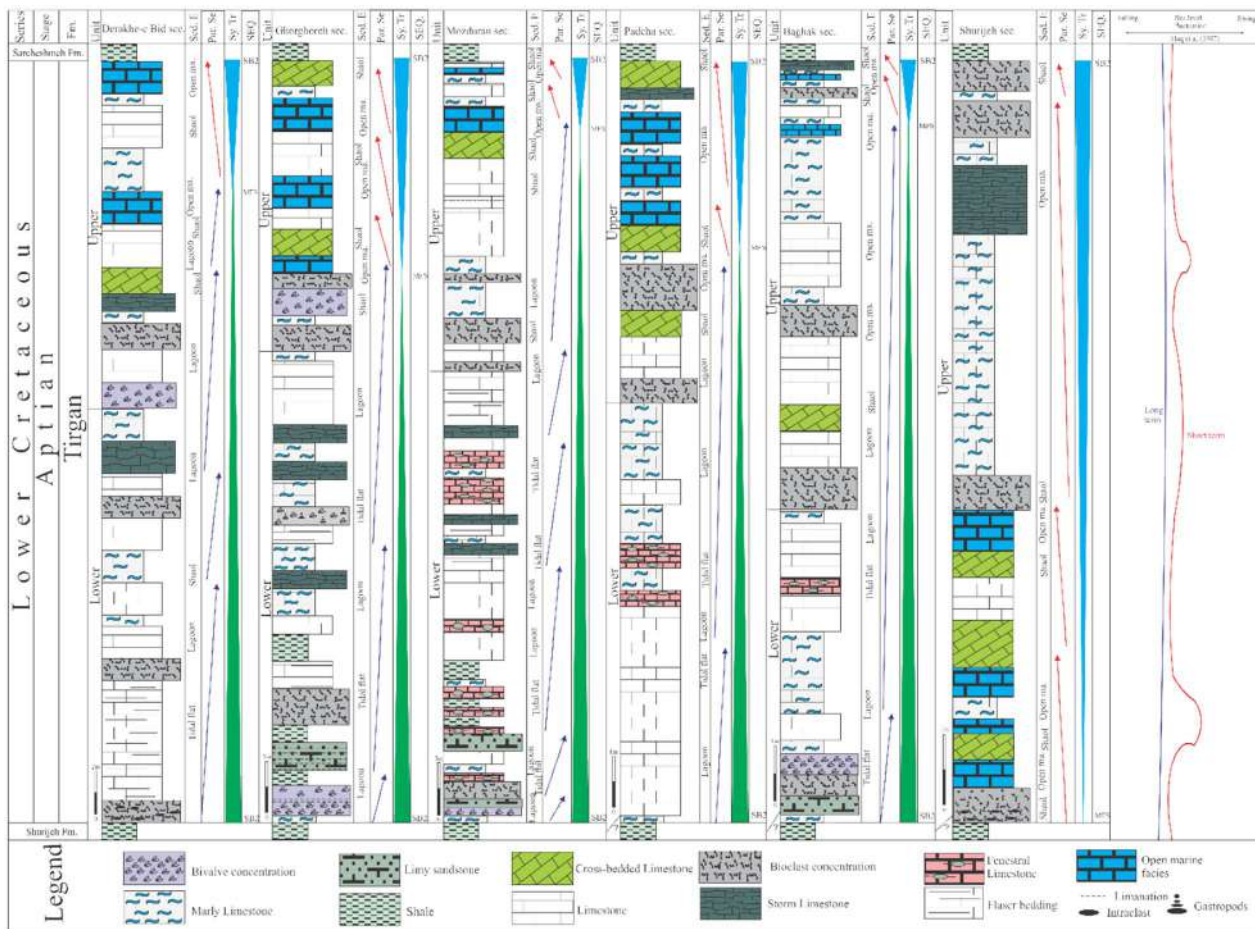


Fig. 14 Lithostratigraphic columns, sedimentary environments (sub-environments), and depositional sequences in the studied sections of the Tigran formation and sea-level fluctuation (Haq et al. 1987). Abbreviations include Sed-E: sedimentary environment; Sy. Tr: Sys-

tem Tracts; SEQ: depositional sequences and sequence boundaries, Par. Se: Parasequence. Vertical scales are different, but for the same scale, please see Fig. 15b

corals. Therefore, field and petrographic investigations and correlation with other sections revealed that was deposited in a carbonate platform of a distal steep ramp type (Fig. 13) during Early Cretaceous. Carbonate sediments were transported off the platform located to the east and south to the west. These resedimented carbonates were transported to the northwest (deepest part of the basin) by turbidity currents. Maximum transgression occurred after deposition of the Tigran formation, the Tigran carbonate platform was drowned and the deep marine facies of the Sarcheshmeh formation was deposited.

Sequence stratigraphy

Base on, field and laboratory studies led to distinguish one depositional sequence in all of the sections, which composes of transgressive, and highstand systems tracts in all of the sections (Fig. 14). This sequence observed in the all

of sections of the west to east of the study area with the presence of 10–30 cm dark gray marly limestone in the most sections and is enclosed by two sequence boundaries SB2, based on underlying intertidal facies and no evidence of exposure, at the bottom and top. The sequence boundary SB2 of this sequence coincides probably with TS (Transgressive Surface) separates the overlying Tigran transgressive deposits from the continental sediments of Shurijeh formation below. Above this boundary TST (Transgressive Systems Tract) deposited in all sections, except the Shurijeh section, the transgressive systems tract (TST) is characterized by open marine, shoal, lagoon, and intertidal facies. Therefore, in the Derakht-e Bid section, the TST starts with Sandy bioclast/oid grain- to rudstone facies with an erosional base oriented finning-upward cycles and with a slightly lateral extension, presence of directing fossils (Fig. 12a), and with distant lateral extension can indicate coastal channels and transgressive evolution, overlain by the lagoon and shoal facies representing retrogradational stacking patterns. The

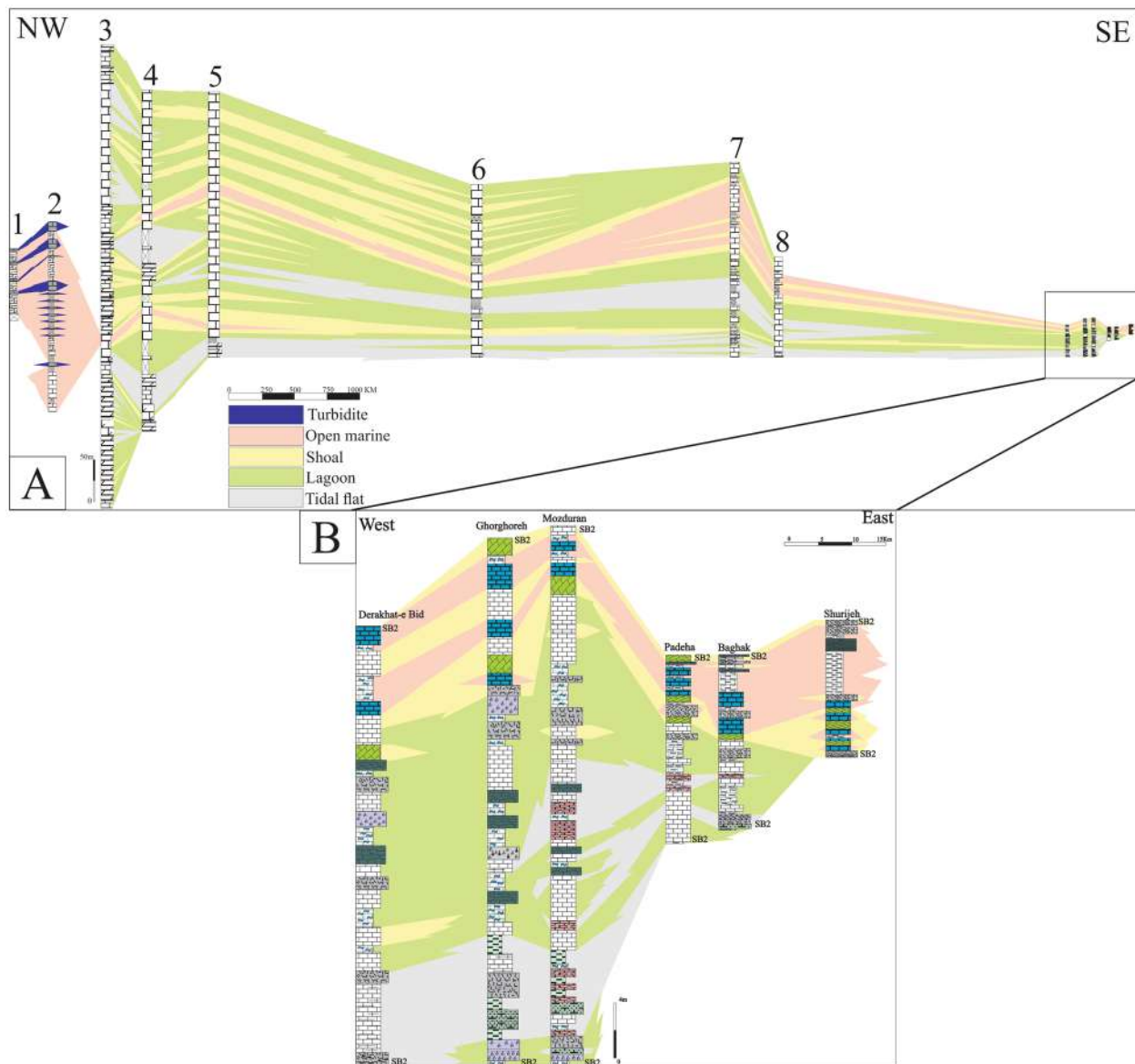


Fig. 15 **a** Correlation of depositional sequences and changes in the vertical and lateral facies belts of the Tirgan formation in the Kopet-Dagh Basin (the numbers sections see Fig. 16). **b** Thickness variation

along with a profile from six sections of the Tirgan formation in the east of Kopet-Dagh Basin

bivalve concentration in the Gorghoreh and Mozduran sections and Baghak sections indicates the transgressive evolution and is located within transgressive system tract. The maximum flooding facies is located on the top of a bioclast peloid grainstone facies in the Derakht-e Bid section and is selected at the top of distal open marine in the Gorghoreh and the Mozduran sections and proximal open marine facies in other sections. Following TST, the highstand systems tract is characterized by the lagoon and open marine setting that reflects an aggradational stacking pattern in all of the sections and consists of shallowing-upward parasequences and is composed of alternation ooid grainstone shoal and ooid

bioclast packstone open marine interlayered with marly limestone (Fig. 14). Due to the uplift basement (Aghdarband tectonic windows), this sequence in the Shurijeh section is suggested as a composite boundary (SB2 + TS + MFS) that HST deposits with bioclast/ooid intraclast grainstone facies directly overlie gray shale of the Shurijeh formation (Fig. 14). The bioclast concentration with an erosional base and normal graded-bedding shallowing-upward cycles, presence of Pebbles with size ranges between 6 to 100 mm (Fig. 12b), cross-lamination and few micro-HCS and randomly oriented was properly occurred in channels created by a storm (Adabi and Rao 1991; Łuczynski et al. 2014). In

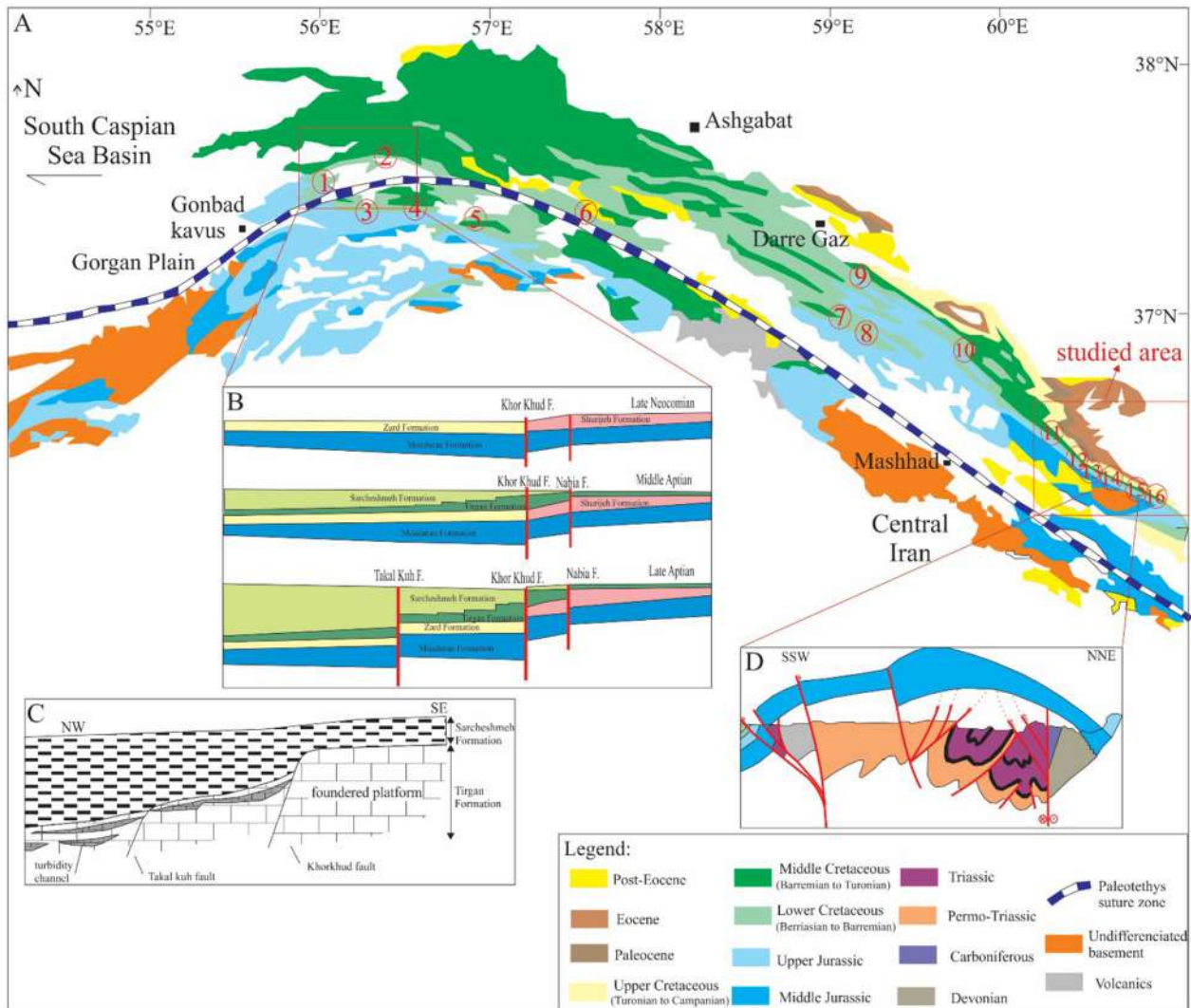


Fig. 16 **a** Simplified geological map of the Kopet-Dagh area compiled from the geological maps of the Geological Survey of Iran. **b** Basement faults of the west Kopet-Dagh were active from the beginning of Cretaceous (Afshar Harb 1979). **c** A schematic profile for the down platform in the west of the basin (Aharipour 1996). **d** Tectonic sketch of the Aghdarband erosional window, modified from previously published cross-sections (Ruttner 1991; Zanchi et al. 2010; Robert et al. 2014). Tectonic sketch of the Aghdarband erosional window, (modified from Ruttner 1991; Zanchi et al. 2010). The num-

bers sections are as follows: 1: the Gharnaveh (80 m thick, Aharipour 1996), 2: the TakelKuh (225 m thick) and 3: the Zav (580 m thick), 4: the Khorkhud (410 m thick), 5: the Jozak (330 m thick) (Tabatabaei 2012), 6: the Sisab (215 m thick, Taher Pour Khalil Abad 2013), 7: Radkan and 8: Chenaran (respectively, 238 and 119 m thick, Javanbakht et al. 2013), 9: the Tirgan (640 m thick, Gheisvand et al. 2019), 10: the Zavin (110 m thick, Javanbakht et al. 2011), 11–16: the study area described above

general, the thickness of this sequence decreases from west to east in the eastern Kopet-Dagh Basin (Fig. 15b).

Discussion and platform evolution

During the Late Cimmerian Orogeny, the non-marine Shurijeh formation deposited in a fluvial setting in the eastern basin and to the west changed gradually to argillaceous calcareous and carbonates marine succession of the Zard formation (Moussavi-Harami and Brenner 1993; Hosseinyar

et al. 2018). With transgression of the Cretaceous sea (late Hauterivian) in central, northwest parts of Kopet Dagh Basin, a thick sequence of carbonate facies of Tirgan formation was deposited extensively (Haq et al. 1987; Haq 2014) that represents one of the Urganian carbonate platforms. Previous studies and our studies of facies analyses by Aharipour (1996), Afshar-Harb (1979), and Tabatabaei (2012) indicate that the Tirgan formation in the village of Tirgan and Khorkhud area is very thick and consists of shallow marine carbonate and decreases to the south (both east and west) and its facies become shallower. The thickness of

this formation decreases to the west but the facies is deepened. As a result, shallow carbonates were formed in the east-southeast and south-west of Kopet-Dagh, due to the activity of Khorkhud and possibly Takalkuh faults (During the Late Cimmerian Orogeny), the carbonate platform in the northwest was gradually subsided (Fig. 16c). This subsidence, coupled with the gradual global sea-level rise, led to the drowning of the platform, slumping and calcareous turbidites (Fig. 15a), (e.g., Gharnaveh section, number 1 in Fig. 16a) could have formed on the continental slope (Aharipour 1996). Also, patch reefs in the outcrops (e.g., Khorkhud section, number 4 in Fig. 16a) (Khazaei 2000) suggest that they formed at the top of the horst blocks of faults (Khorkhud and Takalkuh). At the late Barremian with sea-level rise, the Jozak and Sisab areas (numbers 5, 6 in Fig. 16a) are covered by the shallow sea, and towards the east, it continues onlapping (numbers 7–11 in Fig. 16a) of the basin (Fig. 16b) (Javanbakht et al. 2013; Gheisvand et al. 2019). It is necessary to explain that apparently from the Zavin section towards the Darehgaz area, the thickness of the Tirgan formation increases abruptly. So that, in the Tirgan area, southeast of the town of Darehgaz (number 9 in Fig. 16a), the Tirgan formation has a thickness of 650 m (Gheisvand et al. 2019), while in the Radkan and the Chenaran the thickness is 238 and 119 m, respectively (Javanbakht et al. 2013). So that we suggest that this abrupt increase in the thickness of the Tirgan formation, northeast of the basin, is not related to deposition conditions (e.g., reef builders) and is probably related to the regional tectonics? The sea-level rise at the Aptian, coinciding with the global sea-level rise in Aptian times (Fig. 14) which is called OAE (Oceanic anoxic events), displaced the depositional environments landwards to the east (Kalantari 1969; Immel et al. 1997). During the following transgression systems tract (TST) in the study area that marked with shell beds in the form of transgressive lags within this systems tract. This depositional sequence is the final sea-level fluctuation during the Aptian time in the Tirgan formation that is only recorded central parts and southeast of Kopet-Dagh Basin (Gheisvand et al. 2019). During the following transgression, shallow lagoon and shoal conditions (Fig. 14) was deposited by intraclasts, shell fragments, with sharp erosional bases, poorly sorted is interpreted transgressive lags in TST in the Derakht-e Bid section (number 11 in Fig. 16a) and the Ghorghoreh and the Mozduran sections (numbers 12, 13 in Fig. 16a) in the coastal environment (Fig. 14). This sedimentary sequence also extended in the Padeha and the Baghak sections (numbers 14, 15 in Fig. 16a) but the tidal facies were limited, and most marine facies were deposited (Fig. 14) because of the uplift basement during the Late Jurassic–Early Cretaceous (Aghdarband tectonics window, Ruttner 1991; Zanchi et al. 2010) in this area (Fig. 16d). In this sequence in all of the sections, TST starts with oyster

concentration or bioclast concentration in the form of transgressive lags deposited. These shell beds are interpreted in the base and top of the TST by Kidwell (1991) and Zecchin et al. (2017). Ooid shoal facies with well-preserved fabric that mostly deposited in HST (Fig. 14) reflect LMC (low Mg calcite) mineralogy, seawater chemistry, and Cretaceous rise sea level (Wilkinson et al. 1985; Balthasar and Cusack 2015; Sandberg 1983). Also towards the west, shoals facies (well-sorted ooid grainstone to bioclast peloid grainstone) less energetic than east result the subsidence and increasing depth. The bioclast concentration deposited in all sections probably created by storm currents and interpreted as composite or multi-event concentrations by Kidwell (1991) and Zecchin et al., (2017), which probably concentrate along with the stacking progradational or HST (Nasiri et al. 2019). Tirgan 3-order sequence was possibly developed by Global sea-level fluctuation as the main factor in the study area. Global warming and the overlying of Tirgan formation with deep marine facies of the Sarcheshmeh formation may result in a drowning event during Aptian (e.g., Weissert et al. 1998; Robinson et al. 2017). According to the studies carried out by Taherpour Khalil Abad (2011,2013), all fauna was introduced for the Urganian facies (Renard 1986) as well as lithostratigraphy of these facies (limestone-shale-marl) in the Tirgan formation were identified. So, Base the reconstruction of the environmental conditions of Tirgan formation is relatively similar to the Jura Mountains in Europe of the Urganian platform from the Northern Tethyan margin. In all these regions, evidence of the presence of patch reefs (and thus comparable to some facies of the Tirgan formation) are dated from the Late Barremian, and thus suggest that the installation of Urganian-type facies was a widespread phenomenon within the Tethys.

Conclusion

The sedimentological study and microfacies analysis of the Tirgan formation as part of Urganian platform carbonates, which changed a continental setting into a shallow marine carbonate system, in the Kopet-Dagh Basin improved the understanding of evaluating facies variability and sequence stratigraphic framework. The presence of faults in the northwest suggests that Tirgan formation was deposited in a distally steepened ramp type carbonate platform during Early Cretaceous time. In the northwest basin, slumping and calcareous turbidites could have formed on the continental slope, and patch reefs probably formed at the top of the horst blocks of faults and in Barremian with sea-level rise, the basin are covered by the shallow sea, and towards the east, it continues onlapping. Also, there was local high (Aghdarband tectonics window uplift) during the Late Jurassic–Early Cretaceous time and the last phase of rising sea-level during

Early Aptian time-controlled thickness variations, facies distribution, and deposition of the Tirgan formation the eastern part of Kopet-Dagh. Sequence stratigraphy analysis of this formation in the eastern parts of the basin is a single 3-order depositional sequence in the Derakht-e Bid to Shurijeh sections which is correlated with the Early Aptian global 3-order sea-level cycle. Facies variations with low thickness in the study area probably result in local tectonic (basement uplift) and sea-level rise during Early Aptian and also as the main control of 3-order depositional sequences. Therefore, maximum transgression occurred after deposition of the Tirgan Formation, the Tirgan carbonate platform was drowned (likely global warming during Early Aptian) and the overlying deep marine facies of the Sarcheshmeh Formation was deposited. The microfacies distribution in Tirgan Formation suggests that it is similar over wide areas within the northern Tethyan margin and closer to those of the Jura Mountains.

Acknowledgements This research was supported by the Department of Geology, Ferdowsi University of Mashhad (research code: 3/45360), Iran. The authors thank Dr. Alireza Piriaei and Dr. Mohammad Ali Kavooosi (National Iran Oil Company, Exploration Directorate Tehran, Iran) for his skilled technical assistance. We would like to special thanks to Dr. James W. LaMoreaux, editor-in-chief, Carbonates and Evaporites, and other reviewers of this manuscript for their comments that improved our manuscript significantly.

References

- Abbassi N, Alimohammadian H, Shakeri S, Broumand S, Broumand A (2018) Aptian small dinosaur footprints from the Tirgan formation, Kopet-Dagh region, northeastern Iran. *Bull Am Mus Nat Hist* 80:5–13
- Adabi MH, Rao CP (1991) Petrographic and geochemical evidence for original aragonite mineralogy of Upper Jurassic carbonates (Mozduran Formation), Sarakhs area. *Iran Sediment Geol* 72:253–267
- Adnan A, Shukla UK, Verma A, Shukla T (2015) Lithofacies of transgressive-regressive sequence on a carbonate ramp in Vindhyan basin (Proterozoic): a case of tidal-lat origin from central India. *Arab J Geosci* 8:6985–7001
- Afshar-Harb A (1979) The stratigraphy, tectonics and petroleum geology of the Kopet-Dagh region, northern Iran. Unpublished Ph.D thesis, London: Imperial College of Science and Technology, pp 316
- Afshar-Harb A (1982) Geological map of Sarakhs area. National Iranian Oil Company Geological Division, Tehran
- Aharipour R (1996) Microfacies and depositional environments of the Tirgan, Sarcheshmeh, Pesteh Ligh and Chehel Kman Formations (Lower Cretaceous and Paleocene) in western Kopet-Dagh Basin. MS thesis, Department of Geology, University of Teacher Education, Tehran
- Ahr WM (1973) The carbonate ramp: an alternative to the shelf model. *GCAGS* 23:221–225
- Alavi M (1991) Sedimentary and structural characteristics of the Pale-Tethys remnants in northeastern Iran. *Geol Soc Am Bull* 103:983–992
- Amir Hassan MH, Boon Sim Y, Peng LC, Abdul Rahman AH (2013) Facies analysis of the uppermost Kubang Pasu formation, Perlis: a wave and storm-influenced coastal depositional system. *Sains Malaysiana* 42:1091–1100
- Armella C, Cabaleri NG, Cagnoni MC, Panarello HO (2013) Early Callovian ingress in southwestern Gondwana. Palaeoenvironmental evolution of the carbonate ramp (Calabozo formation) in southwestern Mendoza, Neuquen basin. *Argentina J S Am Earth Sci* 45:293–315
- Arnaud-Vanneau A, Arnaud H (2005) Carbonate facies and microfacies of the lower cretaceous carbonate platforms. In: Adatte T, Arnaud-Vanneau A, Arnaud H, Blanc-Alétru M-C, Bodin S, Carrio Schaffhauser E, Föllmi KB, Godet A, Raddadi MC, Vermeulen J (eds), *The Hauterivian-Lower Aptian sequence stratigraphy from Jura platform to Vocontian Basin: a multidisciplinary approach*, *Géologie alpine Série Spéciale “Colloques et excursions” N7*. pp. 39–68
- Bachmann M, Hirsch F (2006) Lower Cretaceous carbonate platform of the eastern Levant (Galilee and the Golan Heights): stratigraphy and second-order sea-level change. *Cretac Res* 27:487–512
- Bai HQ, Betzler C, Erbacher J, Reolid J, Zuo F (2017) Sequence stratigraphy of upper Jurassic deposits in the North German Basin (Lower Saxony, Süntel Mountains). *Facies* 63:19
- Balthasar U, Cusack M (2015) Aragonite-calcite seas-quantifying the gray area. *Geology* 43:99–102
- Bassi D, Nebelsick JH (2010) Components, facies and ramps: redefining Upper Oligocene shallow water carbonates using coralline red algae and larger foraminifera (Venetian area, northeast Italy). *Palaeogeogr Palaeoclimatol Palaeoecol* 295:258–280
- Betzler C, Brachert TC, Braga JC, Martin JM (1997) Nearshore, temperate, carbonate depositional systems (lower Tortonian, Agua Amarga Basin, Southern Spain): implications for carbonate sequence stratigraphy. *Sediment Geol* 113:27–53
- Bover-Arnal T, Salas R, Moreno-Bedmar JA, Bitzer K (2009) Sequence stratigraphy and architecture of a late Early-Middle Aptian carbonate platform succession from the western Maestrat Basin (Iberian Chain, Spain). *Sediment Geol* 219:280–301
- Brunet MF, Ershov AV, Korotaev MV, Melikhov VN, Barrier E, Mordvintsev DO, Sidorova IP (2017) Late Palaeozoic and Mesozoic evolution of the Amu Darya Basin (Turkmenistan, Uzbekistan). *Geol Soc London* 427:56
- Bucur II, Yarahmadzahi H, Mircescu CV (2019) The Lower Cretaceous Tirgan Formation in the Gelian section (Kopet-Dagh, north Iran): microfacies, microfossil, and their Biostratigraphic significance. *Acta Palaeontologica Romniae* 15:13–33
- Burchette T, Wright V (1992) Carbonate ramp depositional systems. *Sediment Geol* 79:3–57
- Burchette TP, Wright VP, Faulkner TJ (1990) Oolitic sand body depositional models and geometries, Mississippian of southwest Britain: implication in carbonate ramp settings. *Sediment Geol* 68:87–115
- Buryakovskiy LA, Chilingir GV, Aminzadeh F (2001) *Petroleum Geology of the South Caspian Basin*. Gulf Professional Publishing, USA, p 442
- Carevic I, Taherpour Khalil Abad M, Ljubovic-Obradovic D, Vaziri SH, Mirkovic M, Aryaei AA, Stejic P, Ashouri AR (2013) Comparisons between the Urganian platform carbonates from eastern Serbia (Carpatho-Balkanides) and northeast Iran (Kopet-Dagh Basin): depositional facies, microfacies, biostratigraphy, palaeoenvironments and palaeoecology. *Cretac Res* 40:110–130
- Catuneanu O (2006) *Principles of sequence stratigraphy*, 1st edn. Elsevier, Amsterdam, p 375
- Catuneanu O, Abreu V, Bhattacharya JP, Blum MD, Dalrymple RW, Eriksson PG, Fielding CR, Fisher WL, Galloway WE, Gibling MR (2009) Towards the standardization of sequence stratigraphy. *Earth Sci Rev* 92:1–33
- Chatalov A (2013) A Triassic homoclinal ramp from the Western Tethyan realm, Western Balkanides, Bulgaria: integrated insight

- with special emphasis on the Anisian outer to inner ramp facies transition. *Palaeogeogr Palaeoclimatol Palaeoecol* 386:34–58
- Curry BB (1999) An environmental tolerance index for ostracodes as indicators of physical and chemical factors in aquatic habitats. *Palaeogeogr Palaeoclimatol Palaeoecol* 148:51–63
- Davis RA (2012) Tidal signatures and their preservation potential in stratigraphic sequences. In: Davis RA, Dalrymple RW (eds) *Principles of tidal sedimentology*. Springer, Heidelberg, pp 35–55
- Duncan DS, Locker SD, Brooks GR, Hine AC, Doyle LJ (2003) Mixed carbonate-siliciclastic inilling of Neogene carbonate shelf valley system: Tampa Bay, West-central Florida. *Mar Geol* 200:125–156
- Dunham RJ (1962) Classification of carbonate rocks according to depositional textures. In: Ham WE (ed) *Classification of carbonate rocks*. AAPG 1:108–121
- Embry AF, Klovan JE (1971) A late Devonian reef tract on northeastern Banks Island, NWT. *Bull Can Petrol Geol* 19:730–781
- Flügel F (2010) *Microfacies of carbonate rocks analysis, interpretation and application*. Springer, Berlin
- Fursich FT, Oschmann W (1986) Storm shell beds of *Nanogyra virgula* in the Upper Jurassic of France. *Neues Jahrbuch Geol Palaontol Monatsh* 172:141–161
- Gheiasvand M, Föllmi KB, Arnaud Vanneau A, Adatte T, Spangenberg J, Ghaderi A, Ashouri AR (2019) New stratigraphic data for the lower Cretaceous Tirgan formation, Kopet-Dagh Basin, NE Iran. *Arab J Geosci* 12:142–157
- Ghorbani M (2019) *Lithostratigraphy of Iran*. Springer Geology, Cham, p 306
- Haq BU (2014) Cretaceous eustasy revisited. *Global Planet Change* 113:44–58
- Haq BU, Hardenbol J, Vail PR (1987) Chronology of fluctuating sea levels since the Triassic. *Science* 235:1156–1167
- Hosseinyar G, Moussavi-Harami R, Abdollahie-Fard I, Mahboubi A, Noemani-Rad R, Ebrahimi, MH (2018) Facies analyses and depositional setting of the Lower Cretaceous Shurijeh–Shatlyk Formations in the Kopet-Dagh–Amu Darya Basin (Iran and Turkmenistan). *Geol J* 1–15
- Immel H, Seyed Emami K, Afshar-Harb A (1997) Kreide-Ammoniten aus dem iranischen Teil des Koppeh Dagh (NE Iran). *Zitteliana* 21:159–190
- Javanbakh M, Wanas HA, Jafarian A, Shahsavan N, Sahraeyan M (2018) Carbonate diagenesis in the Barremian–Aptian Tirgan formation (Kopet-Dagh Basin, NE Iran): petrographic, geochemical and reservoir quality constraints. *J Afr Earth Sci* 144:122–135
- Javanbakht M, Moussavi Harami R, Mahboubi A (2011) Depositional history and sequence stratigraphy of the Tirgan formation (Barremian–Aptian) in the Zavin section, NE Iran. *IJES* 3:108–118
- Javanbakht M, Ghazi S, Moussavi-Harami R, Mahboubi A (2013) Depositional history and sequence stratigraphy of Tirgan formation (Barremian–Aptian) in central Kopet-Dagh, NE Iran. *J Geol Soc India* 82:701–711
- Kalantari A (1969) Foraminifera from the middle Jurassic–Cretaceous successions of Kopet-Dagh region (NE-Iran) [Unpublished PhD thesis]. London University, Exploration and Production Directorate of NIOC, Geological Laboratory Publication, Tehran 3:298
- Khazaei M (2000) Microfacies analysis and depositional environment of the Tirgan Formation in western Kopet Dagh (southwest of Shirvan-southwest of Bojnord). MS thesis, Department of Geology, Tarbiat-Moallem University, Tehran
- Khodaei MA (1991) Investigation of facies and sedimentary environment of Tirgan Formation (Hauterivian–Lower Aptian) north eastern of Iran. Located in sedimentary Kopet-Dagh Basin and proposing the facies Model. MS thesis, Department of Geology, University of Teacher Education, Tehran
- Kidwell SM (1991) Condensed deposits in siliciclastics sequences: expected and observed features. In: Einsele G, Ricken W, Seilacher A (eds) *Cycles and events in stratigraphy*. Springer, Berlin, pp 682–695
- Laya JC, Tucker ME (2012) Facies analysis and depositional environments of Permian carbonates of the Venezuelan Andes: Palaeogeographic implications for Northern Gondwana. *Palaeogeogr Palaeoclimatol Palaeoecol* 331:1–26
- Łuczynski P, Skompski S, Kozłowski W (2014) Stromatoporoid beds and flat-pebble conglomerates interpreted as tsunami deposits in the Upper Silurian of Podolia, Ukraine. *Acta Geol Pol* 64:261–280
- Miall AD (1997) *The geology of stratigraphic sequences*. Springer, Berlin
- Molaei M, Vaziri SH, Raisossadat SN, Taherpour-Khalil-Abad M, Taheri J (2019) Late Barremian–early Aptian Ammonites from the Tirgan formation, Kopet-Dagh Sedimentary Basin, NE Iran. *J Sci* 30:51–59
- Moussavi-Harami R, Brenner RL (1990) Lower Cretaceous (Neocomian) fluvial deposits in eastern Kopet Dagh Basin, northeastern Iran. *Cretac Res* 11:163–174
- Moussavi-Harami R, Brenner RL (1992) Geohistory analysis, petroleum reservoir characteristics of lower Cretaceous (Neocomian) sandstones, eastern Kopet Dagh Basin, northeastern Iran. *AAPG* 76:1200–1208
- Moussavi-Harami R, Brenner RL (1993) Diagenesis of non-marine petroleum reservoirs: the Neocomian (lower Cretaceous) Shurijeh formation, Kopet Dagh Basin, NE Iran. *J Petrol Geol* 16:55–72
- Nasiri Y, Moussavi-Harami R, Mahboubi A, Mosaddegh H (2019) Sequence stratigraphic significance of shell concentrations in the Mobarak formation (Mississippian), Aloorz Zone, Northern Iran. *N Jb Geol Palaont Abh* 2:171–195
- Nelson CS, Keane SL, Head PS (1988) Non-tropical carbonate deposits on the modern New Zealand shelf. *Sediment Geol* 60:71–94
- Palma RM, Lopez-Gomez J, Piethel RD (2007) Oxfordian ramp system (La Manga formation) in the Bardas Blancas area (Mendoza Province) Neuquén Basin, Argentina: facies and depositional sequences. *Sediment Geol* 195:113–134
- Payros A, Pujalte V, Tosquella J, Orue-Etxebarria X (2010) The Eocene storm-dominated foralgal ramp of the western Pyrenees (Urbasa-Andia formation): an analogue of future shallow-marine carbonate systems. *Sediment Geol* 228:184–204
- Perez-Lopez A, Perez-Valera F (2012) Tempestite facies models for the epicontinental Triassic carbonates of the Betic Cordillera (southern Spain). *Sedimentology* 59:646–678
- Pomar L (2001) Types of carbonate platforms: a genetic approach. *Basin Reserve* 13:313–334
- Purkis SJ, Harris PM (2016) The filling and patterns of sediment filling of accommodation space on Great Bahama Bank. *J Sediment Res* 86:294–310
- Read JF (1985) Carbonate platform facies models. *AAPG* 69:1–21
- Renard M (1986) *Chimisme de l’Ocean, Phenomenes Geodynamiques Internes et Evolution de la Biosphere. Application a la Crise Barremienne: “La Naissance de l’Ocean Moderne”/Oceanic Chemism, Internal Geodynamic Phenomena and Biosphere Evolution. Application to the Barremian Crisis: “The Creation of the Modern Ocean”* (from: *Bulletin des Centres de Recherches Exploration-Production elf aquitaine* 10: 593–606
- Robert AMM, Letouzey J, Kavooosi MA, Sherkat S, Muller C, Verg-ees J, Aghababae A (2014) Structural evolution of the Kopet Dagh fold-and-thrust belt (NE Iran) and interactions with the South Caspian Sea Basin and Amu Darya Basin. *Mar Petrol Geol* 57:68–87
- Robinson SA, Heimhofer U, Hesselbo SP, Petrizzo MR (2017) Mesozoic climates and oceans a tribute to Hugh Jenkyns and Helmut Weissert. *Sedimentology* 64:1–15
- Rubert Y, Jati M, Loisy C, Cerepi A, Foto G, Muska K (2012) Sedimentology of re-sedimented carbonates: facies and geometrical characterisation of an upper Cretaceous calciturbidite system in Albania. *Sediment Geol* 257:63–77

- Ruttner A (1991) The Triassic of Aghdarband (AgDarband), NE-Iran, and its pre-Triassic frame. *Abhandlungen der Geologischen Bundesanstalt* 38:252
- Sandberg PA (1983) An oscillating trend in Phanerozoic non-skeletal carbonate mineralogy. *Nature* 305:19–22
- Sharafi N (2012) Facies, depositional environment, and sequence stratigraphy of the Tirgan Formation in western Kopet Dagh. PhD thesis, Department of Geology, Islamic Azad University Science and Research Branch, Tehran
- Singh BP (2012) How deep was the early Himalayan foredeep? *J Asian Earth Sci* 56:24–32
- Stöcklin J (1977) Structural correlation of the Alpine ranges between Iran and Central Asia. *Memoire Hors Serie No 8 de la Société Géologique de France* 8:333–353
- Tabatabaee P, Lasemi Y, Jahani D (2018) Facies variability of a lower Aptian carbonate platform succession, Tirgan Formation, eastern Kopet Dagh Basin, northeast Iran. *Carbonates Evaporites* 1–12
- Tabatabaee P (2012) Facies, depositional environment, and stratigraphy of the Tirgan and Shurijeh Formations, in central and eastern Kopet Dagh. PhD thesis, Department of Geology, Islamic Azad University Science and Research Branch, Tehran
- Taherpour Khalil Abad M, Aryaei AA, Ashouri AR, Ghaderi A (2011) Introducing some echinoderms from the Tirgan formation, Kopeh-Dagh Basin, NE of Iran. *Geopersia* 1:83–94
- Taherpour Khalil Abad M, Schlagintweit F, Vaziri SH, Aryaei AA, Ashouri AR (2013) *Balkhania balkhanica* Mamontova, 1966 (benthic foraminifera) and *Kopetdagaria sphaerica* Maslov, 1960 (dasycladalean alga) from the Lower Cretaceous Tirgan formation of the Kopet Dagh mountain range (NE Iran) and their paleobiogeographic significance. *Facies* 59:267–285
- Tamura T, Masuda F (2003) Shallow-marine fan delta slope deposits with large-scale cross-stratification: the Plio-Pleistocene Zaimokuzawa Formation in the Ishikari Hills, northern Japan. *Sediment Geol* 158:195–207
- Vail PR, Audemard F, Bowman SA, Eisner PN, Perez-Cruz C (1991) The stratigraphic signatures of tectonics, eustasy and sedimentology: an overview. In: Einsele G, Ricken W, Seilacher A (eds) *Cycles and events in stratigraphy*. Springer, Berlin, pp 617–659
- Van Wagoner JC, Mitchum RM, Campion KM, Rahmanian VD (1990) Siliciclastic sequence stratigraphy in well logs, cores, and outcrops. *AAPG* 7:55
- Weissert H, Lini A, Follmi KB, Kuhn O (1998) Correlation of early Cretaceous carbon isotope stratigraphy and platform drowning events: a possible link. *Palaeogeogr Palaeoclimatol Palaeoecol* 137:189–203
- Wilkinson BH, Owen RM, Carroll AR (1985) Submarine hydrothermal weathering, global/eustasy, and carbonate polymorphism in Phanerozoic marine oolites. *J Sediment Petrol* 55:171–183
- Wilson JL (1975) Carbonate facies in geologic history. Springer, Berlin, p 471
- Yavarmansh H, Vaziri H, Aryaei AA, Jahani A, Pourkermani M (2017) Microfacies and morphotectonic of the Tirgan formation in Ghorogh syncline (North of Chenaran). *Int J Geogr Geol* 6:79–93
- Zanchi A, Balini M, Ghassemi MR, Zanchetta S (2010) Mechanism of calcrete formation in the lower Cretaceous (Neocomian) fluvial deposits, northeastern Iran based on petrographic, geochemical data, EGU General Assembly
- Zanchi A, Zanchetta S, Balini M, Ghassemi MR (2016) Oblique convergence during the Cimmerian collision: evidence from the Triassic Aghdarband Basin, NE Iran. *Gondwana Res* 38:149–170
- Zecchin M, Caffau M, Catuneanu O, Lenaz D (2017) Discrimination between wave-ravinement surfaces and bedset boundaries in Pliocene shallow-marine deposits, Crotone Basin, southern Italy: an integrated sedimentological, micropaleontological and mineralogical approach. *Sedimentology* 64:1755–1799

Publisher's Note Springer Nature remains neutral with regard to jurisdictional claims in published maps and institutional affiliations.